

**Paleo Arctic Ocean Hydrograph and Circulation in
Last Glacial Maximum as Obtained from NAOSIM
Model**

MSc. Thesis

*Group Paleoclimate Dynamics, AWI
Key Laboratory of Marine Environment and Ecology, OUC
Post Graduate Program Environmental Physics, Uni-Bremen*

Xun Gong

2009

Research Guides: Pro. Dr. Gerrit Lohmann & Pro. Dr. Ruediger Gedert

Acknowledgements

Special thanks to Prof. Dr. Gerrit Lohmann and Prof. Dr. Ruediger Gedert for their constant support, never-ending patience, and spot-on guidance. No lesser thanks to Dr. Frank Kauker, Dr. Michael Karcher and Cornelia Koeberle for their techniques supports. I would also like to thank Axel Waganer, who is a genius group member, and helped me persevere through some of the tougher times. And I am ever indebted to the supports from my Chinese colleagues and families.

Contents

1. Introduction

1.1 Overview

1.2 The roles of Arctic Ocean in the Earth climate system

1.2.1 Arctic Ocean

1.2.2 Earth's climate and Arctic Ocean

1.3 Last Glacial Maximum

1.4 Objectives

2. Theoretical framework

2.1 General equations of fluid motion

2.1.1 Assumptions and definitions

2.1.2 Mass conservation in the ocean

2.1.3 Momentum conservation in the ocean

2.2 The dynamics and thermodynamics of sea ice

2.2.1 The dynamics of sea ice

2.2.2 The thermodynamics of sea ice

3. Numerical framework

3.1 Model description

3.2 Model set up

3.2.1 Present experiments

3.2.2 LGM surface forcing experiments

3.2.3 Experiments

4. Results and discussion

4.1 Paleo ocean circulation in LGM

4.1.1 Arctic Ocean circulation in LGM

4.1.2 Nordic seas & Arctic Ocean circulation in LGM

4.2 Sea ice distribution and drift

5. Conclusions

6. Bibliography

1. Introduction

1.1 Overview

To set the scene for our studies, we begin with what we know about the terrain distribution and climate conditions between today and Last Glacial Maximum (LGM) in Arctic Ocean regions. We then concentrate on the circulation in the Arctic Ocean, and introduce its importance to the global climate system and what we know about its influence mechanisms. Our aim is to study this circulation using numerical tools that help us to understand the underlying processes that are associated with it. Our tool of choice is North Atlantic-Arctic Ocean Sea Ice Model (NAOSIM), and therefore, we describe the problems faced with such models, and present the state of the art. Since our aim is to understand the Arctic Ocean circulation during the LGM, we start from very basics of fluid dynamics. While much of its initial sections are often considered to be rather standard in the scientific community, its careful and stepwise formulations helped me understand, connect and assess the variety of approaches in the model. It also paves the way for the critical analysis of present and LGM circulation. Then, we address the numerical aspects of the model framework and its actual implementation forcing conditions. Finally, we proceed to present and discuss some of our results, also describe some of diagnostic data to test and confirm our model results.

The thesis is formulated in the following way:

In section 1, the basic characteristics and conditions of the Arctic Ocean (in section 1.2), the features of LGM time slice(in section 1.3) are briefly introduced.

In section 2, the theoretical frameworks are presented by general equations of fluid motion (in section 2.1), and the mechanisms of sea ice formation and melting (in section 2.2) are given.

In section 3, we describe NAOSIM model, and the initial and forcing data we prepared for the model.

In section 4, the model experiments performed and the results obtained are presented (in section 4.1). Some previous works and arts about paleo biological and geological evidences are described in section 4.3. With this background information at hand, we

then proceed to clearly and specifically outline the objectives of our work.

In section 5, we conclude with a brief summary of our results and further steps to be taken.

1.2 The roles of Arctic Ocean in the Earth climate system

1.2.1 Arctic Ocean

The Arctic Ocean is one of five major oceanic divisions, which takes 2.8% of Earth's total surface area, about 14,056,000 km² [1]. It is surrounded by the continents of Eurasia, North America, Greenland and some other islands. Along the Eurasia land mass line, the ocean is divided into Chukchi Sea, Eastern Siberian Sea, Laptev Sea, Kara Sea, Barents Sea, Greenland Sea, Norwegian Sea, and within its western part, are Beaufort Sea, Baffin Bay, Hudson Bay, Iceland Sea and Labrador Sea.

The average depth of the Arctic Ocean is 1,038m. The Lomonosov Ridge divides the North Polar Basin into Eurasian Basin and American Basin, both of them are over 4,000m depth. The deepest point of the whole Arctic basin is in the 5,450 m Eurasian Basin. The bathmetric map is shown in Fig.1.

The basic stratification of the Arctic Ocean consists of an upper mixed layer (30–50m), halocline complex layer (50–200m), intermediate depth layer (200-1,000m), and deepwater (>1,000m)[2][3].The Pacific surface current goes into the Arctic Ocean through Bering Strait, through the layer between 50m and 200m. The North Atlantic water penetrates to the Arctic via Fram Strait and St. Anna Trough (Barents Sea), then under extensive cooling, which sinks to intermediate depth (approximately 200–800m deep)[4]. In the experiments, we focus on no deeper than 1,000m depth of Arctic Ocean. Regionally, it can be ascribed to a number of processes that related circulation pattern to Atmosphere influence, the input of fresh water, warm ocean currents, melting and freezing of sea ice.

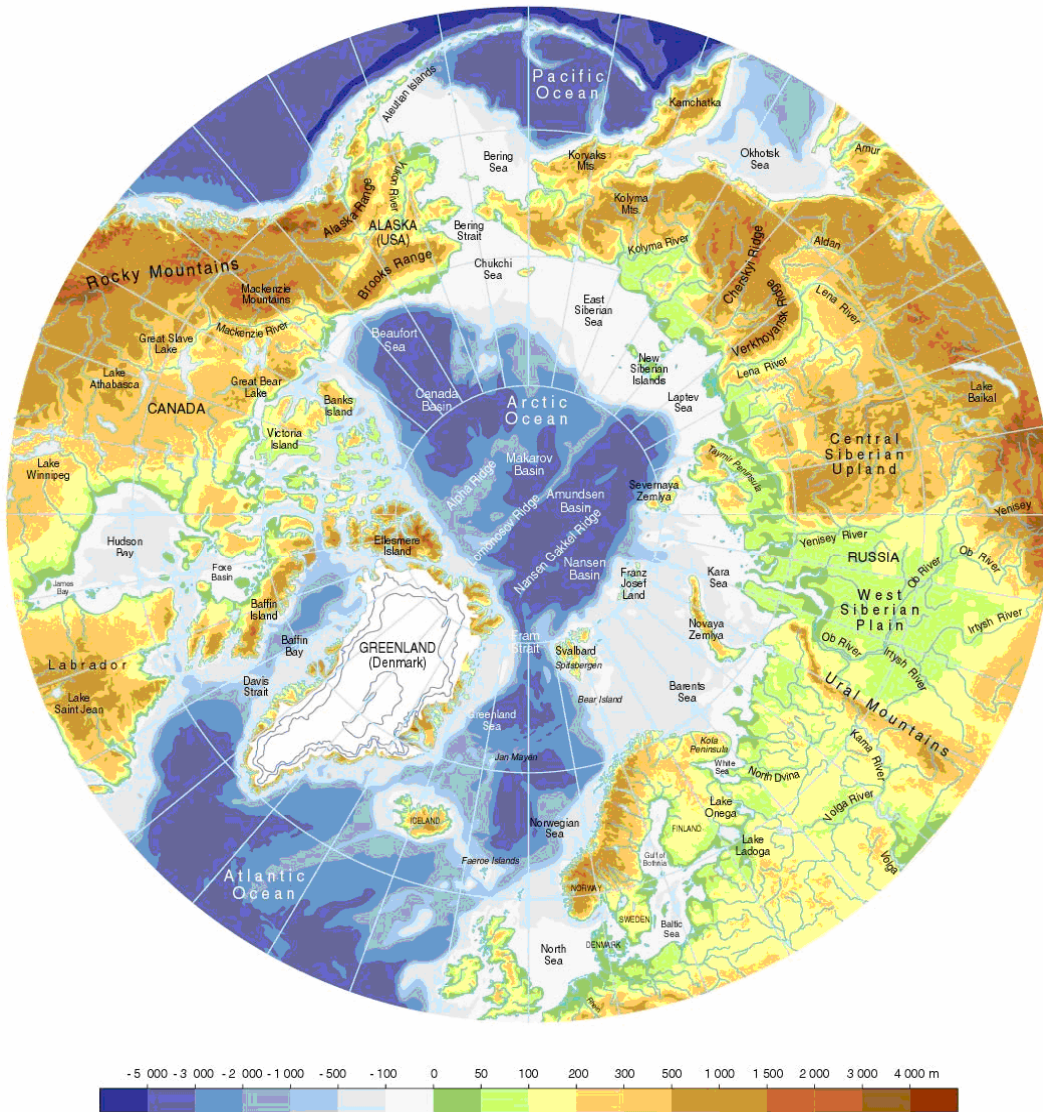
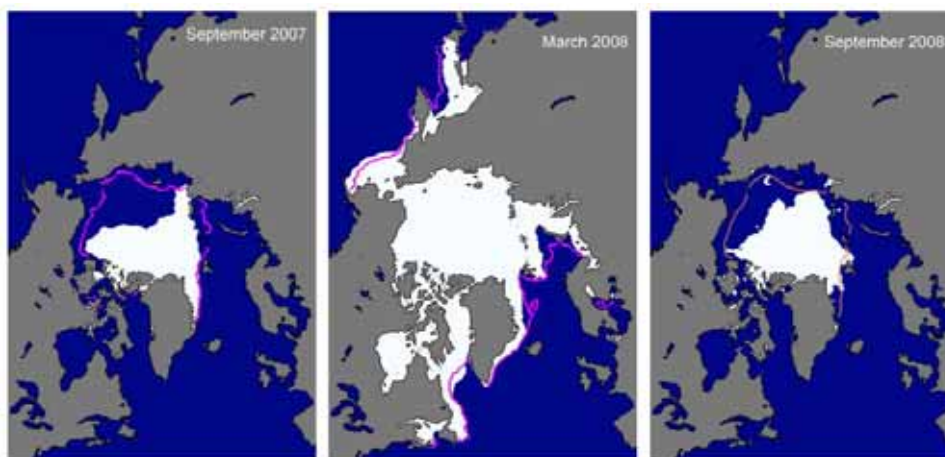


Fig.1 Topography and bathymetry of the Arctic (based on the ETOP5 data set), AMAP (Arctic Monitoring and Assessment Programme, 2005)



(a)

(b)

(c)

Fig.2 Sea ice distribution in September 2007 (a), March 2008 (b) and September 2008 (c), illustrating the respective winter maximum and summer minimum extents. The magenta line indicates the median maximum and minimum extent of the ice cover, for the period 1979–2000. The September 2007 minimum extent marked a record minimum for the period 1979–2008. From the National Snow and Ice Data Center Sea Ice Index: [nsidc.org/data/ seaice_index](http://nsidc.org/data/seaice_index).

The fresh water balance of the Arctic Ocean is determined by three major inputs and the ocean export of ice and water. The inputs are as follows: river discharge, precipitation minus evaporation (P-E) and the transfer of low-salinity ocean water, primarily through the Bering Strait. These three contributions are in the approximate proportions of 2:1:1[5]. The major rivers entering the Arctic Ocean comprise an area of over 22,000 km² and drain watersheds extending as far south as about 45°N[6]. Individual contributions from the major rivers entering the Arctic Ocean are shown schematically in Fig.3., including the Yenisei (630 km³yr⁻¹), Lena (532km³yr⁻¹), Ob (404km³yr⁻¹), Pechora (130km³yr⁻¹), Kolyma (128km³yr⁻¹), Severnaya Divna (109km³yr⁻¹), Khatanga (88km³yr⁻¹), and Indigirka (54km³yr⁻¹) from Eurasia, and Mackenzie (262km³yr⁻¹) and other gauged rivers (209km³yr⁻¹) in North America. River runoff is clearly one of the key processes contributing to the Arctic Ocean's circulation, which has prompted consideration of an estuarine-like circulation for the Arctic Ocean, and simple models reflecting this view have been proposed[7] [8].

The other fresh water storage reservoirs of the Arctic Ocean are ice sheet and sea ice. There are huge ice sheet in the Greenland and Novaya Zemlya Island (in Barents Sea), but the ice shrinks 19 cubic miles per year in Arctic region. The extent of the sea ice cover is typically at or near its maximum in March and its minimum in September. The ice extent in March 1979-2008 was 14.4 million km², and 6.7 million km² in September. Data from submarine based observation indicates that, the sea ice thickness thinned by an average of 1.3m between 1956-1978 and 1990-2005[9].

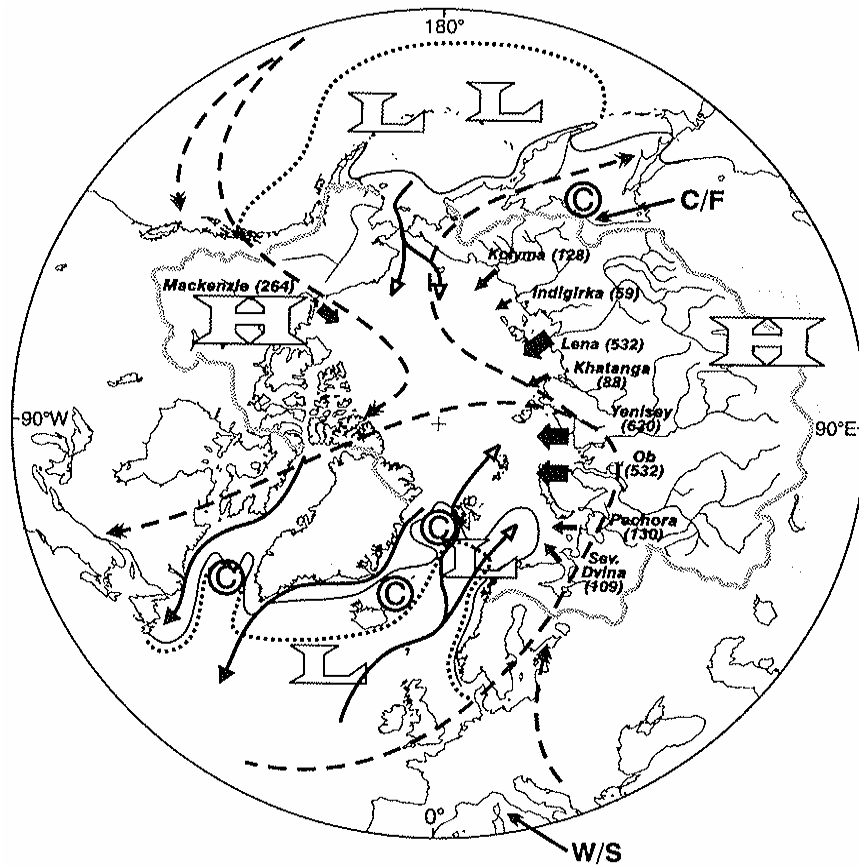


Fig.3 Present Arctic river distributions. There are 7 rivers in the Eurasia continent, and 1 river injection from the North American continent.

The climate of the Arctic is described by repeating patterns of sea level pressure (SLP) that can dominate individual months or can represent the overall atmospheric circulation flow for an individual winter or spring season term. The main pattern is known as the Arctic Oscillation (AO) circulation regime, which is widely considered as the main source of Arctic climate variability during the twentieth century. A second pattern influences from Pacific sector to the Arctic is the Pacific North American (PNA) pattern. A positive period of the AO has lower sea level pressure over the central Arctic, brings warmer temperatures to Eurasia, and helps export sea ice into Atlantic Ocean. [10] [11]

1.2.2 Earth's climate and Arctic Ocean

It is currently thought that the Arctic Ocean impact on global climate by regulating deepwater formation rates, relate to the Meridional Overturning Circulation (MOC). If

the MOC is driven vigorously in high northern latitudes, the northern European climate is moderate; on the other hand, if overturning diminishes, the climate cools dramatically.

The strength of the overturning circulation, and thus the oceanic heat transport, is determined by the ocean density distribution, especially the vertical structure at high latitudes. The horizontal exchange and convection between the North Atlantic Ocean and the Arctic Ocean is in the Greenland and Iceland seas. If the exporting fresh water from the Arctic Ocean were to increase, the northward extension of Atlantic water would retreat, and the convective regions would shift a bit south, MOC would likely be diminished. Conversely, if the supply of fresh water were to decrease, and stratification within the Arctic Ocean to decrease, a shift northwards of the convective regime might be expected, and the climatological ice cover would spread southward, then MOC would become more vigorous [12] [13].

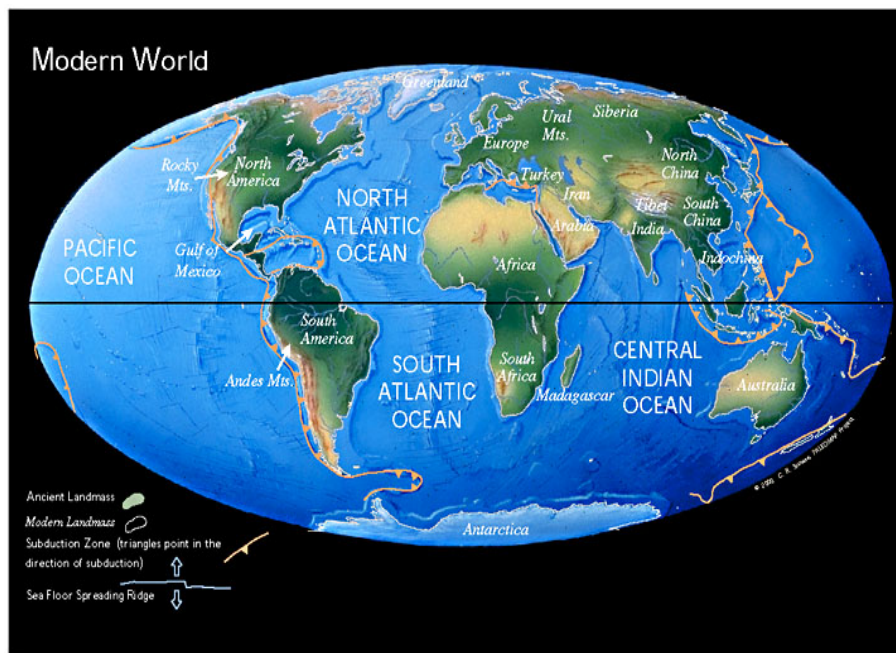
In addition to the global ocean hydrological cycle, the high latitudes part of cryosphere is also a dominant element to the earth's climate change, and most of them are distributed in the high latitudes. There are 5 patterns: ice sheet, ice shelves, glacier, sea ice, snow, and you can find all components in Arctic region, especially the sea ice. In contrast to others, sea ice doesn't originate from fresh water, but mostly from the sea water. An initial cooling in the polar regions, with a larger sea ice extent, will induce further cooling through the less absorbing the solar energy, by the increased global albedo. The water albedo is only 4%-15%, but the ice surface could reach 60%. This process is so-called 'Temperature-ice-albedo feedback'.

The unique physical features of sea ice, also influence in the dynamics and thermodynamics process between atmosphere and ocean. The salinity of sea water is about 34.7 psu, but sea ice only contains 5 psu. The brine water produced in ice formation is very important to deep water formation.

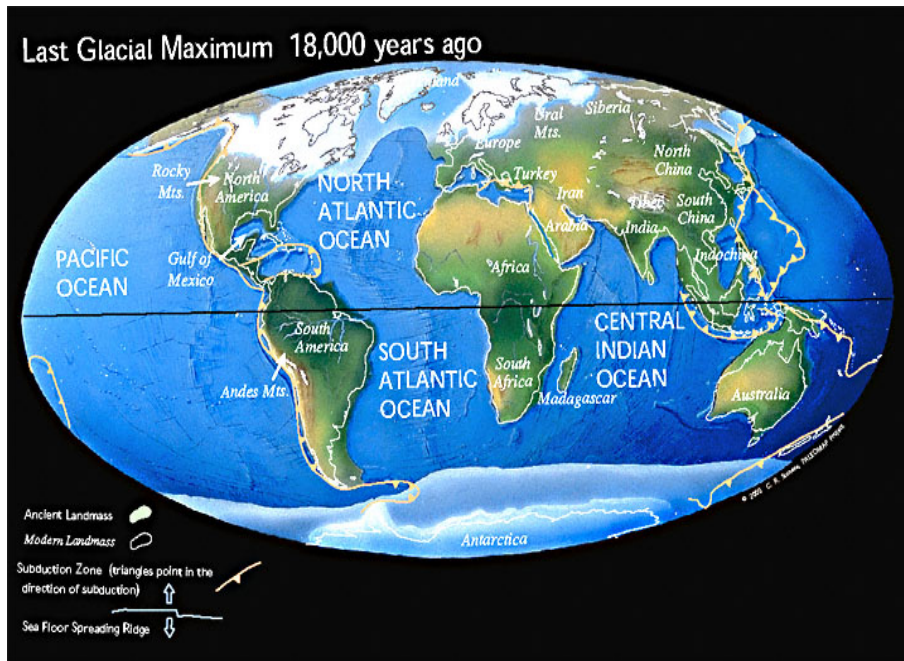
1.3 Last Glacial Maximum

The last glacial period (LGP) began about 110,000 years ago and ended between 10,000 and 15,000 B.P.. The evidences of paleoclimatological records are different

from region to region, but the maximum extent of glaciations was approximately 20000 years ago. The most important signal link to the climate is the global mean temperature, which could reflect the overall planetary energy balance. But it's difficult to determine the global mean cooling during LGM. Proxy data from ice and sediment cores only provide the local information. The numerical estimates to the global mean temperature differs by 3 to 6°C, due to the input forcing conditions and the models themselves [14]. LGM is characterized by the maximum ice sheet volume in northern hemisphere ice sheets. Canada, as well as the northern part of USA, was nearly completely covered by land ice, and blanketed by the huge Laurentide ice sheet. But Alaska remained mostly ice free due to arid climate conditions. On the Europe and north-western Asia mainland, the Scandinavian ice sheet reached the northern part of the British Isles, Germany, Poland and Russia, also extended east to the Taimyr Peninsula in western Siberia. North-eastern Siberia was not covered by a continental-scale ice sheet. According to the sediment composition retrieved from deep ocean, there must even have been times of seasonally open waters [15] [16] [17] [18]. Climate at the LGM were cooler and almost everywhere drier. Rainfall could be diminished by up to 90% in glaciated areas of Europe and North America. Even in less affected regions, the florals line retreated obviously.



(a)



(b)

Fig.4 Global ice sheet distribution map of the present (a) and LGM (b), from PALEOMAP Project, 2001. There is obviously difference in Polar Regions between the glacial and interglacial periods.

2. Theoretical framework

2.1 General equations of fluid motion

2.1.1 Assumptions and definitions

Thin-shell approximation

The depth of global ocean is a few thousand meters, and the average earth radius is about 6.378×10^6 meters. Within the same latitude and longitude on the earth, the gravitational acceleration and Coriolis force's difference between different ocean vertical layers is no more than 0.1%. That is usually ignored in the calculations.

Rigid-lid approximation

In numerical models, we usually make an approximation that, vertical displacements of the ocean surface are not allowed, i.e. ignoring the sea surface height variations, as being covered with a rigid surface on top of the ocean.

$$\frac{\partial H_0}{\partial t} = -\left(\frac{\partial U}{\partial x} + \frac{\partial V}{\partial y}\right) = 0$$

Where, H_0 is the sea surface height, U & V are the vertical integration of horizontal velocity from sea surface to bottom.

Density of sea water

The variations of density determine the distribution of pressure inside the ocean, and then influence the ocean currents. The density depends on the salinity, temperature and the pressure, an anomaly of density is usually calculated by a non-linear equation:

$$\sigma(S, t, p) = \rho(S, t, p) - 1000 \text{ kg/m}^3 \quad \text{or} \quad \sigma_t = \rho(S, t_p, 0) - 1000 \text{ kg/m}^3$$

Where, S , t and p are the salinity, temperature and pressure, t_p is the potential temperature, and σ_t is called potential density.

Wind stress

Wind stress is a horizontal drag force of the wind on the sea surface, by which the momentum is transferred from the atmosphere to the ocean vertically. It is calculated from:

$$T = \rho C_D U_{10}^2$$

Where, ρ is the density of air, U_{10} is wind speed at 10 meters, and C_D is the drag coefficient.

Vertical mixing in the ocean

Vertical mixing requires more energy than horizontally in the ocean, due to the buoyancy mechanism. A vertical mixing would change the vertical density structure, then the ocean currents and circulations, which is described as:

$$\frac{\partial \Theta}{\partial t} + W \frac{\partial \Theta}{\partial t} = \frac{\partial}{\partial z} \left(A_z \frac{\partial \Theta}{\partial z} \right) + S$$

Where, Θ is a tracer, A_z is the vertical eddy diffusivity, which depends on the pressure and potential temperature, and S is tracer sources.

2.1.2 Mass conservation in the ocean

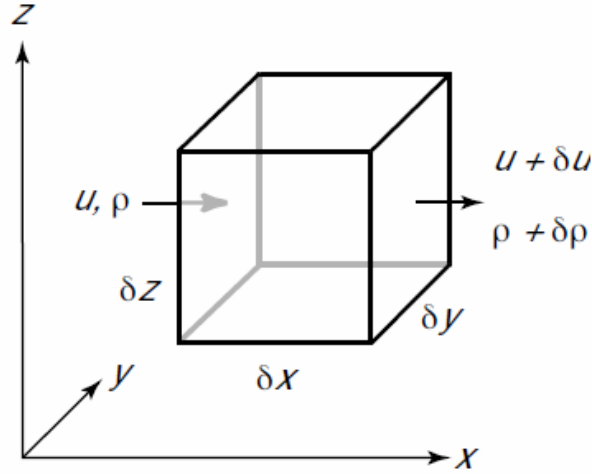


Fig.5 The mass flux for continuity equation.

In the X direction, a mass flow into and out of the cube:

$$Flow_{in}^x = \rho u \delta y \delta z$$

$$Flow_{out}^x = (\rho + \frac{\partial \rho}{\partial x} \delta x)(u + \frac{\partial u}{\partial x} \delta x) \delta y \delta z$$

Then, the mass flux is

$$Flux^x = Flow_{out}^x - Flow_{in}^x$$

$$= (\rho + \frac{\partial \rho}{\partial x} \delta x)(u + \frac{\partial u}{\partial x} \delta x) \delta z \delta y - \rho u \delta y \delta z$$

$$= (\rho \frac{\partial u}{\partial x} + u \frac{\partial \rho}{\partial x} + \frac{\partial \rho}{\partial x} \frac{\partial u}{\partial x} \delta x) \delta x \delta y \delta z$$

Because of $\delta x \rightarrow 0$, the third term is much smaller than the former 2 terms, i.e.

$$[\frac{\partial \rho}{\partial x} \frac{\partial u}{\partial x} \delta x] \ll [\rho \frac{\partial u}{\partial x}], [\rho \frac{\partial u}{\partial x}], \text{ so,}$$

$$Flux^x \approx \frac{\partial(\rho u)}{\partial x} \delta x \delta y \delta z$$

In all three dimensions X, Y, Z :

$$Flux^{x,y,z} = (\frac{\partial(\rho u)}{\partial x} + \frac{\partial(\rho v)}{\partial y} + \frac{\partial(\rho w)}{\partial z}) \delta x \delta y \delta z$$

In the selected volume, the change of mass is:

$$Mass_{local} = \frac{\partial \rho}{\partial t} \delta x \delta y \delta z$$

So, the mass conservation equation:

$$0 = Flux^{x,y,z} + Mass_{local}$$

$$\left[\frac{\partial \rho}{\partial t} + \frac{\partial(\rho u)}{\partial x} + \frac{\partial(\rho v)}{\partial y} + \frac{\partial(\rho w)}{\partial z} \right] \delta x \delta y \delta z = 0$$

$$\frac{\partial \rho}{\partial t} + \frac{\partial(\rho u)}{\partial x} + \frac{\partial(\rho v)}{\partial y} + \frac{\partial(\rho w)}{\partial z} = 0$$

$$\frac{1}{\rho} \left(\frac{\partial \rho}{\partial t} + u \frac{\partial \rho}{\partial x} + v \frac{\partial \rho}{\partial y} + w \frac{\partial \rho}{\partial z} \right) + \frac{\partial u}{\partial x} + \frac{\partial v}{\partial y} + \frac{\partial w}{\partial z} = 0$$

$$\frac{1}{\rho} \frac{D\rho}{Dt} + \frac{\partial u}{\partial x} + \frac{\partial v}{\partial y} + \frac{\partial w}{\partial z} = 0$$

2.1.3 Momentum conservation in the ocean

In the Cartesian coordinate system, the momentum equation is

$$\frac{\partial u}{\partial t} + u \frac{\partial u}{\partial x} + v \frac{\partial u}{\partial y} + w \frac{\partial u}{\partial z} = -\frac{1}{\rho} \frac{\partial p}{\partial x} + 2\Omega v \sin \varphi + F_x$$

$$\frac{\partial v}{\partial t} + u \frac{\partial v}{\partial x} + v \frac{\partial v}{\partial y} + w \frac{\partial v}{\partial z} = -\frac{1}{\rho} \frac{\partial p}{\partial y} - 2\Omega u \sin \varphi + F_y$$

$$\frac{\partial w}{\partial t} + u \frac{\partial w}{\partial x} + v \frac{\partial w}{\partial y} + w \frac{\partial w}{\partial z} = -\frac{1}{\rho} \frac{\partial p}{\partial z} + 2\Omega u \cos \varphi - g + F_z$$

Where, F_i are the components of any frictional force per unit mass, and φ is

latitude; the pressure term p is calculated by:

$$dp = \rho(S, T, p_0) g dz$$

Where, S, T are the temperature and salinity, p_0 is the sea surface pressure.

2.2 The dynamics and thermodynamics of sea ice

2.2.1 The dynamics of sea ice

The following sea ice equations describe the relation between ice/snow velocity and forcing factors: the Coriolis force, surface ocean tilt, air and water stress, and internal ice stress.

$$\frac{du}{dt} = fv - g \frac{\partial \zeta_w}{\partial x} + \tau_a^x + \tau_w^x + F_x$$

$$\frac{dv}{dt} = -fu - g \frac{\partial \zeta_w}{\partial y} + \tau_a^y + \tau_w^y + F_y$$

$$\bar{\tau}_a = \rho_a C_a |\vec{V}_{10}| \vec{V}_{10}$$

$$\bar{\tau}_w = \rho_w C_w |\vec{v}_w - \vec{v}| (\vec{v}_w - \vec{v})$$

Where, $g \frac{\partial \zeta_w}{\partial x}$ is the tilt effect by the surface ocean water, τ_a is the wind stress, τ_w is the ocean current stress, F is the internal stress within ices.

2.2.2 The thermodynamics of sea ice

The characteristic features to describe the sea ice melting and formation are the ice thickness and ice concentration:

$$\frac{DAh_i}{Dt} = \frac{\rho_o}{\rho_i} [A(W_{io} - W_{ai}) + (1-A)W_{ao} + W_{fr}]$$

$$\frac{DA}{Dt} = \frac{\rho_o A}{\rho_i h_i} [\Phi(1-A)W_{ao} + (1-A)W_{fr}] \quad 0 \leq A \leq 1$$

The term Ah_i is the effective thickness, which is simply quantifying the change in the amount of ice. It is influenced by the melt rate on the upper ice/snow surface W_{ai} , the freeze rate at the air/water interface W_{ao} , rate of frazil ice growth W_{fr} , and freeze rate at the ice/water interface W_{io} .

3. Numerical framework

3.1 Model description

Our simulating experiments are upon a coupled ocean-sea ice model of the NAOSIM (North Atlantic/Arctic Ocean-Sea Ice Model), which is hierarchy developed at Alfred Wegener Institute for Polar and Marine Research [21] [22].

In the model, the ocean part derives from the Geophysical Fluid Dynamics Laboratory modular ocean model MOM-2 [23]. A biharmonic diffusion of momentum is depicted by a horizontal diffusion coefficient of $-0.5 \times 10^{21} \text{cm}^4 \text{s}^{-1}$, and the constant friction

coefficient for vertical viscosity is taken as $10\text{cm}^2 \text{ s}^{-1}$. On the sea bed, the drag coefficient is set to 1.2×10^{-3} of the bottom drag coefficient. For some advected tracers, such as potential temperature, salinity, a FCT scheme is characterized by a low implicit diffusion while avoiding false extrema (“overshooting”) [24] [25]. The barotropic horizontal velocities normal to the boundary are specified from a lower-resolution version of the model that covers the whole North Atlantic Ocean, but the baroclinic velocities are calculated from a simplified momentum balance [26]. The prognostic variables within the ocean model are potential temperature, salinity, velocity, wind stress, stream function, convection depth, and heat flux between the atmosphere and sea surface.

Coupled with the oceanic part, the dynamic & thermodynamic sea ice modules employ a viscous-plastic rheology [27] [28]. The thermodynamics process is described by Semtner (1976) [29]. There are 5 variables calculated: ice thickness, ice concentration, ice drift velocity, snow thickness, and heat flux. By solving the energy budget equation for a single ice layer with optional snow cover, the mass of ice freezing and melting are calculated, independently from salinity.

Etopo5 data set of National Geophysical Data Center is used to the ocean topography, but it is a modification by opening two channels in the Canadian Archipelago to the Arctic Ocean in Baffin Bay [30]. The model domain area includes the Arctic Basin, Nordic Seas, part of North Atlantic Ocean, and the north part of Eurasia and America continents. The southern ocean boundary is 50°N . The other ocean boundaries in present time (i.e. Bering Strait, the Kattegat, and Hudson Strait) are closed. Besides outflows of tracers and the radiation of waves [31], it is also open for the sea ice drift. And a 180 days towards a yearly mean constant of climatology temperature and salinity is restored in boundary stream function [32] [33].

NAOSIM is set onto a spherical rotated grid of $0.25^\circ \times 0.25^\circ$ resolution, and unevenly spaced 30 levels. To shift the realistic equator to the geographical 30°W median and North Pole to the (0°N , 60°E), this transformation in different coordinates as following:

$$\begin{cases} geolat(i, j) = \max(-\frac{\pi}{2}, \min(90.0, \arcsin(\cos(mlat(i, j)) \times \cos(mlong(i, j)))))) \\ geolon(i, j) = \text{mod}(\frac{11}{6}\pi + \left| \frac{\arccos(\cos(mlat(i, j)) \times \sin(mlon(i, j)) \times \cos(mlon(i, j)))}{\cos(\arcsin(\cos(mlat(i, j))))} \right|, 2\pi) \end{cases}$$

Where, $geolat(i, j)$ & $geolon(i, j)$ are geographical latitude and longitude, and $mlat(i, j)$ & $mlon(i, j)$ are North-south and East-west coordinate in the model.

The initial forcing, such as potential temperature and salinity, comes from the Arctic Ocean EWG climatology for winter [34]. Levitus and Boyers (1994) and Levitus et al. (1994) climatology data are used in where the model domain exceeds the EWG climatology area. The atmosphere forcing conditions involves daily mean 2m air temperature, 2m dew point temperature, total cloud cover, net precipitation, sea surface wind speed and wind stress.

3.2 Model set up

3.2.1 Present experiments

In the present experiments, the daily mean atmospheric data is from NCEP/NCAR reanalysis within the time via 1948 to 2007 [35]. A restoring flux for accounting the river runoff from continents, and the inflows through Bering Strait is added to the surface freshwater flux (with an adjustment timetable of 180 days). The river flow is calculated in reference to observed data from the EWG-atlas [34] for the Arctic Ocean and Nordic Seas. And Levitus and Boyers (1994) and Levitus et al. (1994) for the rest of the model area [22].

3.2.2 LGM surface forcing experiments

Compared with the present time slice, the atmosphere status, ocean circulation and land-oceans-glaciers distribution during LGM period are different in LGM. New forcing and boundary conditions were reset for the 20 kyr BP simulations.

Land-sea mask - The geological surveys about ice sheet imply that the sea level was about 120m lower during LGM as a result of growth of ice sheets, and more Arctic region was covered by ice sheet [36]. The Bering Strait and north Siberian tundra steppe were covered by a huge ice sheet. Then the warm and less salty Pacific Ocean

water would not enter the Arctic Basin. The Innuitian Ice Sheet on the Queen Elizabeth and Ellesmere Islands connected the North American continent and the Greenland Island together, the exchange between the Beaufort Sea and Baffin Bay disappeared. In the Eurasia continent, a huge land ice sheet in LGM will cover the entire Kara Sea and the north Barents Sea, also involving the west Siberian Plain, North Russian, Norwegian area. Base on the present ocean bottom topography (Etopo5 data set of National Geophysical Data Center), the sea level was subtracted by 120m, and the land ice sheets were added in the above mentioned Eurasia areas. Then, the narrowed Fram Strait became the most important and only existed passageway linking the Arctic Ocean with the rest of global ocean environment, where the mass and momentum could exchange [37] [38] [39] [40] [41].

Paleo rivers – In the primary expectation, freshwater discharge is very important to general the circulation model simulation. But actually, there are still many arguments about the river routine and the amount of runoff in each river. Some further unknowns behind these , are the runoffs seasonal variations and how the possible existing paleo proglacial lakes would influence the freshwater discharges. Base on some geological peleo results and some related model simulations, we believe that, there are 3 paleo rivers directly flowing into the Arctic Ocean in the LGM. The estuary of Paleo Eurasia River (P-1 River) is on the LGM ice sheet margin of Laptev Sea area, and a proglacial lake would be at the Kara Sea, due to a probably 800 m height ice sheet mountain there [42]. The East Siberian tundra plain was only covered by sporadic ice sheet in LGM, for a extremely dry atmosphere circulation there, the discharge of paleo Lena River (Paleo-2 River) are considered more than the P-1 River, due to a wider freshwater source area [43] [44]. In LGM, North American continent was covered by land ice sheet, but the paleo Mackenzie River (Paleo-3 River) routine area, i.e. the north-west part of Alaska, was still free of ice-sheet [36], and the river discharge was not much less than today by the estimate of the balance between melt water and precipitation in North America continent in LGM, in spite of small flux disbalance due to continental lake storage [45].

time step and the equal 30 days in each month of 15 years. Because of the $0.25^{\circ} \times 0.25^{\circ}$ resolution in NAOSIM, an interpolation from T42 to model resolution has been done with an interpolation radius of 500 km.

Paleo ocean boundary – the ocean boundary is 50°N in the North Atlantic Ocean and Labrador Sea, and the realistic circulation is still unknown in this area. The sensitivity analysis of the Atlantic Ocean is also a part of the target of simulations. Base on the present model ocean boundary, a half stream function, 2 degree higher temperature and 1 psu plus salinity are implied in different experiments at the southern model boundary.

Furthermore, according to the salinity conservation, plus 1 psu salinity is assumed in the entire ocean body in the model domains area.

3.2.3 Experiments

To reconstruct the paleo-ocean circulation and sea ice distribution in LGM, 9 experiments are set in different forcing conditions.

Tab.1 Experiments NAOSIM Model Simulation

No.	Run	Forcing Condition				
		Atmosphere	Land-Sea Mask	Runoff	Salinity	50°N Ocean
A.	PALEO	NCEP	LGM	-	S	S, T, V
B.	PALEO_2	NCEP	LGM	PALEO	S	S, T, V
C.	PALEO_3	NCEP	TODAY	TODAY	S	S, T, V
D.	LGM	LGMO	LGM	-	S+1	S, T, V
E.	LGM_2	LGMO	LGM	PALEO	S+1	S, T, V
F.	LGM_3	LGMG	LGM	PALEO	S+1	S, T, V
G.	LGM_4	LGMO	LGM	PALEO	S+1	S+1, T-2, V/2
H.	LGM_5	LGMO	LGM	PALEO	S+1	S+1, T-2, V
I.	LGM_6	LGMO	LGM	PALEO	S+1	S, T, V/2

Under the present atmosphere forcing condition, Experiment A & B are expected to reveal the contributions of paleo land-sea mask and paleo rivers in LGM. All the conditions in Experiments C are in present time slice, so it provides a control run. The geological evidence of paleo rivers in LGM is still very limited. Experiment D & E are set with & without paleo freshwater discharge into Arctic basin. Compared with polar areas, the physical properties of climate and ocean in the tropics and subtropics regions during LGM are still unknown. The sea surface forcing in Experiment F is of LGMG, which is warmer than the LGMO condition in the North Atlantic Ocean. Some assumptions about the T, S and momentum inflow on the southern boundary of model domain area are set to test the sensitivities from North Atlantic Ocean.

4. Results and discussion

4.1 Paleo ocean circulation in LGM

4.1.1 Paleo Arctic Ocean circulation in LGM

In modern interglacial time period, the Arctic Ocean is well connected with the global oceans: the Pacific warm current flows into Arctic Ocean; in the wide-open Fram Strait and Barents Sea area, a strong water mass and energy exchange between the North Atlantic Ocean and Arctic Ocean happen there; and the Labrador current transports a branch of Arctic upper layer water into the Atlantic Ocean, which is very important to the meridional ocean circulation. Perennially strong stratification could be found in the central Arctic Ocean, but the Beaufort gyre has a seasonal variability due to the monthly changing wind stress.

In Experiments E, we set all the input forcing as what it should be in LGM slice. During LGM, the nearly closed Arctic Ocean was only open to the Atlantic Ocean through Fram Strait, the Barents Sea, Kara Sea and Bering Strait were covered by the land ice or blocked by enlarged Siberian plain cause of the 120m lower sea level. The average sea surface salinity is 32.6, which is about 1psu higher than the modern time. There is nearly no variation of sea surface temperature in the central Arctic Ocean, which is around -1.74°C , a bit warmer than the critical sea ice formation temperature -1.8°C . The thermohaline layer is up to 800m, from 50m depth.

The maximum temperature and salinity could be found at the layer from 850m to 1050m. The average temperature in the intermediate layer of LGM is -0.15°C , which is 0.2 degree than the present.

While performing the outcomes of the experiments, we choose some sections and points in the model area to discuss the hydrographic features, Fig.7.

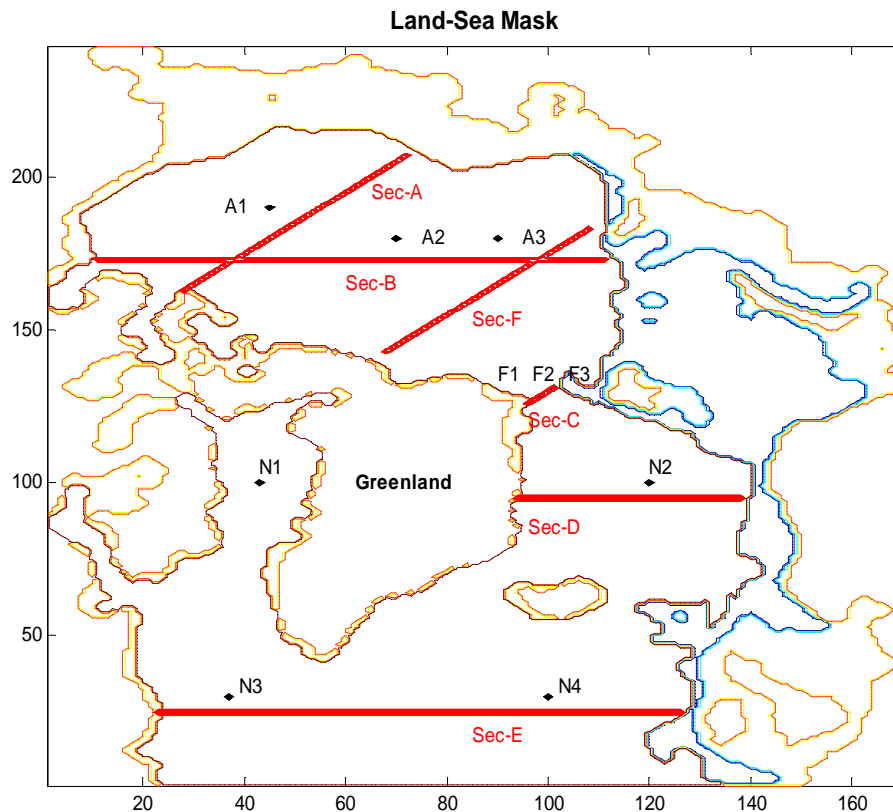
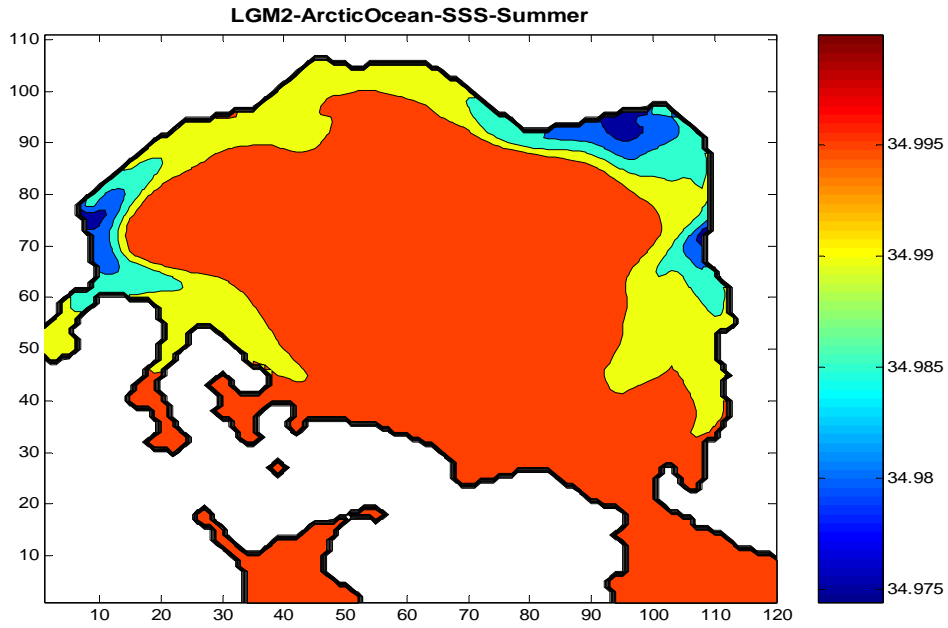
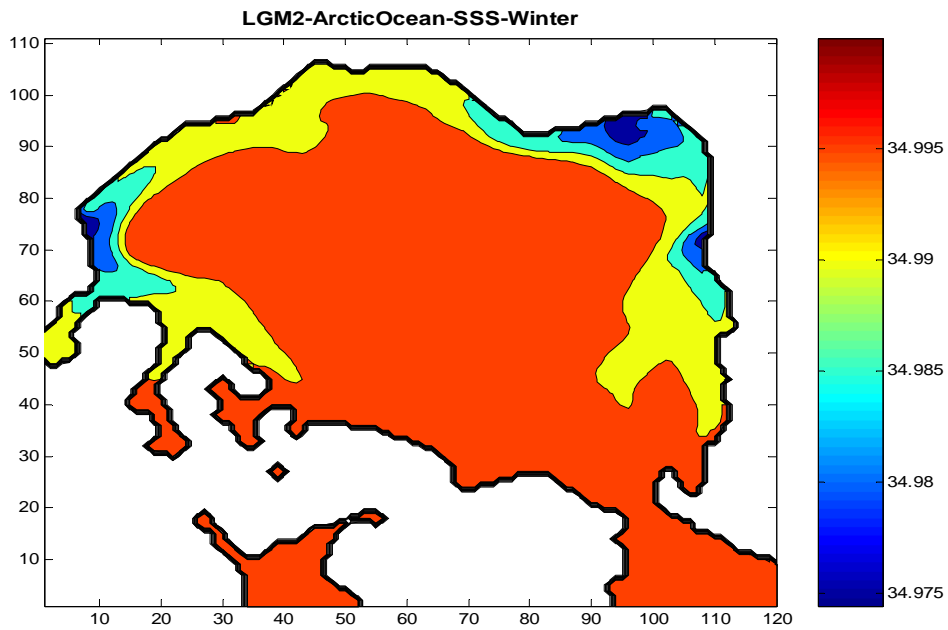


Fig.7 We choose 3 vertical sections (Sec-A, Sec-B & Sec-F) and 3 example points (A1, A2 & A3) in Arctic Ocean, and 2 sections (Sec-D & Sec-E) and 4 example points (N1, N2, N3 & N4) in the area of Nordic Seas and North Atlantic Ocean to visualize and analysis the thermocline and halocline structure of the ocean. In the previous evaluation for model outcomes, Fram Strait is a key entrance or exit for the Arctic Ocean water exchange, Sec-C is just across the whole channel, and F1, F2 & F3 are selected to visualize the details of possible difference of it.



(a)



(b)

Fig.8 Winter/Summer difference of Arctic Ocean sea surface salinity in LGM. Fig.8-a is the value of multi-year average of June, July and August for summer season; and Fig.8-b is mean value of December, January and February of multi-years.

Fig.8 shows the obtained results of sea surface salinity (SSS) in Arctic Ocean during the summer and winter term of LGM. There is no obvious change of the horizontal salinity distribution in the first upper layer of the ocean, in winter and summer. Salinity decreases from the central to the coast, the annual mean of centre is about always 34.99. We can clearly see the influence of fresh water discharge from the paleo rivers around the Arctic Basin. The fresh water lies on the shelf and flows along the isobath lines. Because of the strong stratification, the fresh water could not sink into the very deep layer, actually the influence is only limited within no more than upper 150m depth.

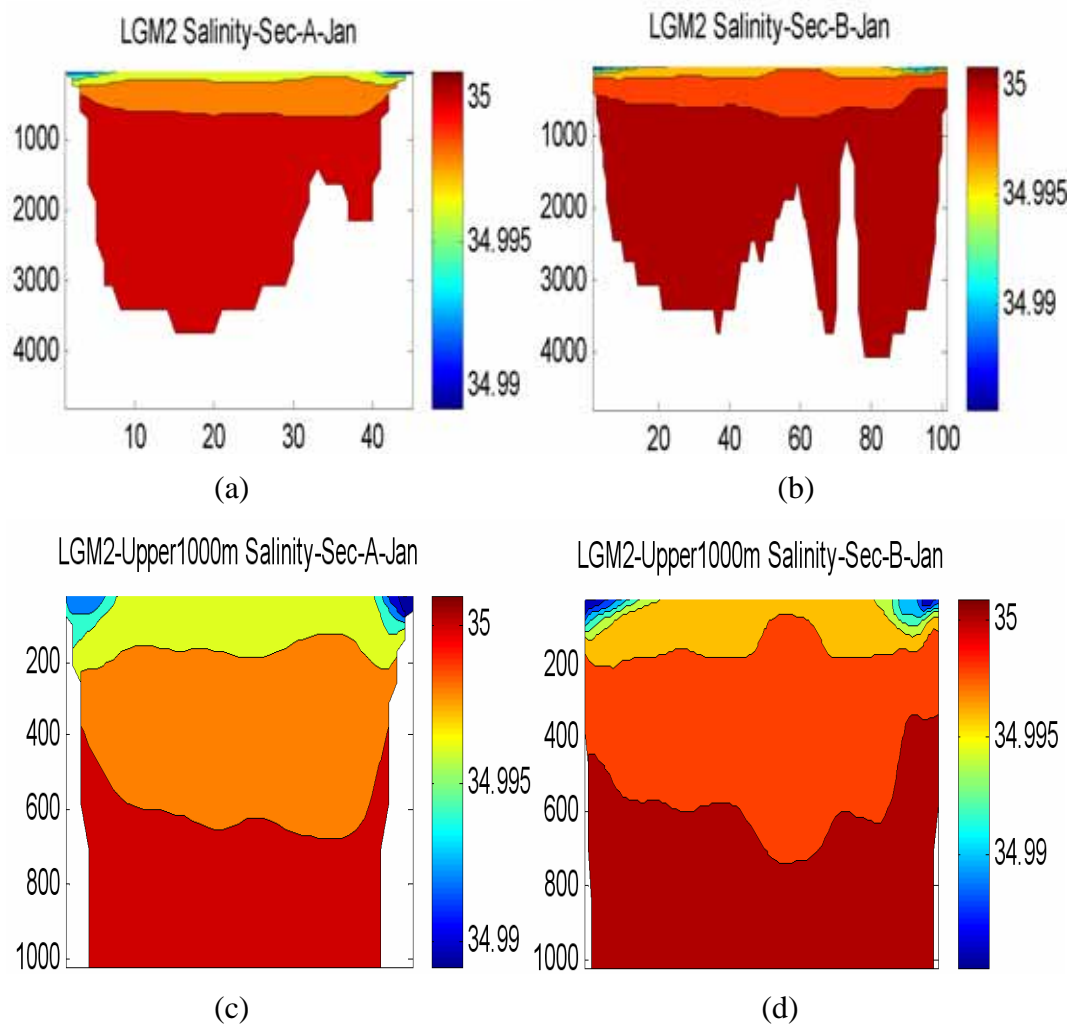


Fig.9 The vertical salinity structure of the Section A and Section B. Fig.9-a & b show the status in Experiment E, and Fig.9-c & d perform only the upper 1000m of the ocean.

The image of Salinity in Fig.9 is the vertical halocline structure of Section A (Fig.9-a) and Section B (Fig.9-b) from the Experiment E. Salinity increases from the surface to the bottom, with a scale of 0.005 psu, there are 3 layer, lower than 1,000m depth, the water mass could be taken as a stable and constant body in decades years. The bottom of intermediate layer is about 1,000m, similar as present. Even though strong stratification, the difference between the surface layer and deep layer water is only 0.01 psu. Fig.9-c and d perform only the first 1,000m of Section A and B under the set up of Experiment E. In these images, the rivers are only obtained on the boundary of the basin; the deepest impact depth is in about 150m. Fig.9-e and f are the upper 1,000m of Section A and B from Experiment D. The halocline is much smoother and hierarchy, but the intermediate layer doesn't change. Compared with the E, Experiment D has no river injections into the Arctic Ocean. So, in spite of the paleo river influence to the central Arctic Ocean is not obviously available in Fig.9, we still can find the evidences from fresh water to the central ocean water mass on the at least 600m depth.

In the following images Fig.10, we could see the profiles of selected points A-2 & A-3. The blue solid line stand for the temperature features, and the red dashed line shows the salinity. In Fig.10-a & b, we assume that we lose paleo rivers, but the images Fig.10-c & d are from the LGM control run. Between Fig.10-a & c, they are nearly the same; and this is also between the Fig.10-b & d. So, it is clear that, the river runoff doesn't change the vertical salinity and temperature features of Arctic Ocean, during LGM. Due to the perennial ice coverage, the sea surface temperature is always constant at around -1.8 degree, which is the ice-water formation balance temperature in the model. Within the same temperature forcing but different fresh water runoff into the ocean, the thermodynamic equilibrium could change, i.e. the efficiency of ice-formation would be different. So, in the Fig.10-a, the sea surface salinity is 32.7, 0.2 psu lower than Fig.10-c, that might because the local thermodynamic influence or from the different water mass transported by ocean currents only due to the dynamic process of the paleo rivers' injection.

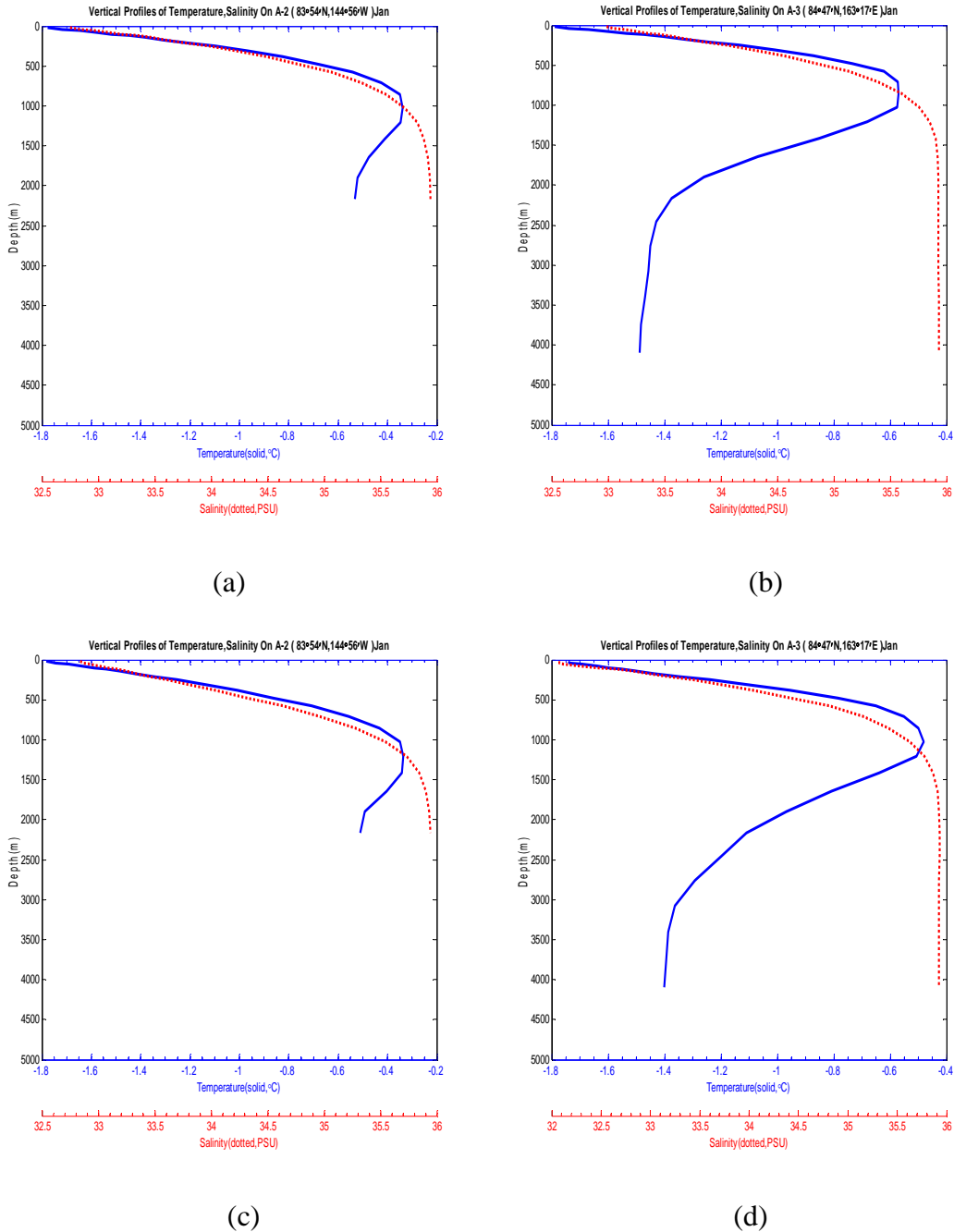


Fig.10 The vertical salinity and temperature profiles of the points A-2 and A-3. Fig.10-a & b show the vertical structure of Experiment D, i.e. without the paleo river injection, and profiles in the Fig.10-c & d are from Experiment E.

NAOSIM model is well sea ice-ocean coupled, and involves the fresh water forcing from the land. So as a previous expects, the sea surface currents, i.e. in the first 20m depth of the ocean, would be the currents containing the dynamic and thermodynamic impacts from the sea ice and fresh water discharge. In numerical simulation, the

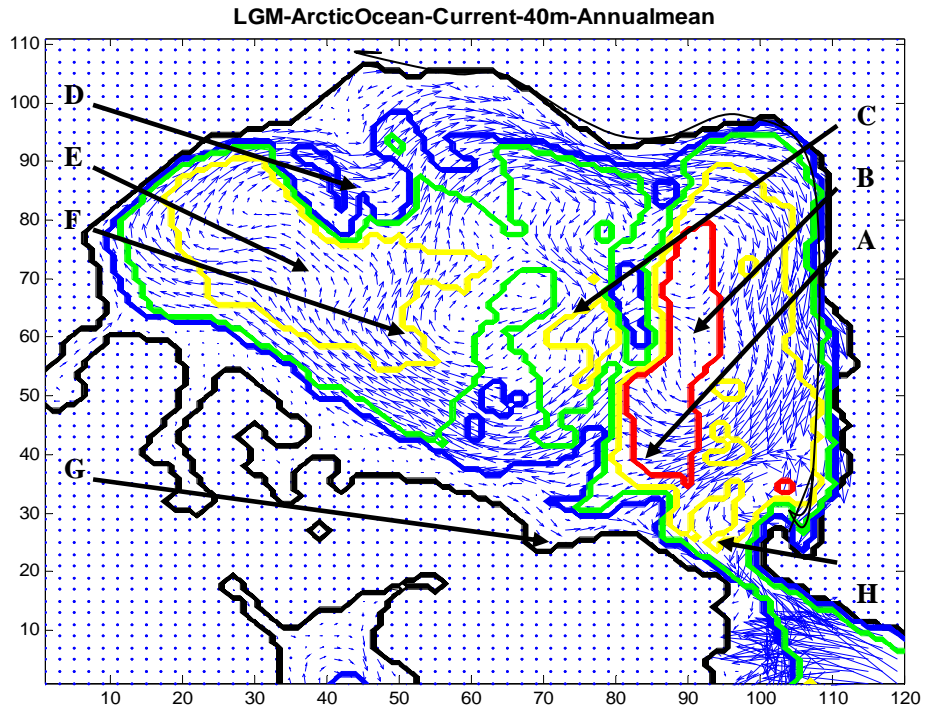
influence of sea ice and ocean to each other only locate in the first layer (20m depth). But from Fig.9 & 10, we could see the fresh water could reach the about 150m, 7th layers. To isolate the basis ocean currents and the effects from different factors, we could discuss the ocean circulations as following, in Tab.2

Tab.2 Analysis for sea surface ocean currents

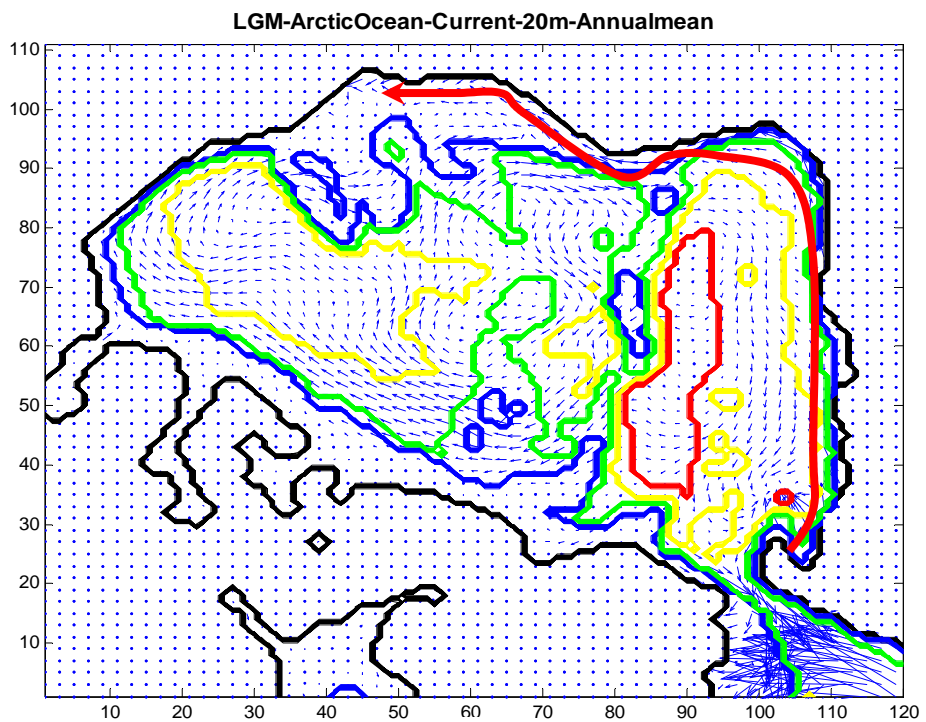
	Experiments and layer	Model outcomes
Step 1	Experiment D, 2nd layer	Basic sea surface ocean currents
Step 2	Experiment D, 1st layer	Basic sea surface ocean currents & Sea Ice effect
Step 3	Experiment E, 2nd layer	Basic sea surface ocean currents & River effect
Step 4	Experiment E, 1st layer	Realistic sea surface ocean currents in LGM
Step 5	Experiment E & F, 1st layer	The impact from atmosphere forcing
Step 6	Experiment E & H, I, 2nd layer	The impact of North Atlantic Water

Step 1

Fig.11-a shows obtained result for Arctic Ocean circulation at 40m depth within the set up of Experiment D. This pattern could be regarded as from all the LGM forcing conditions by the paleo fresh water discharge and sea ice influence. There is a strong anticyclone circulation along the coastline. Above the Eurasia basin (the red isobath line of 3500m), the coastal current make two clockwise curves at the position A & B, and turn to the central Arctic area. At the position C, it performs an 'S' curve there, and by the ocean topography, we can find a sea bed rise (small green close line of 2000m depth) at the north-east and south-west of the 'C'. The 'S' stream line at C and the curves at A & B are caused by potential vorticity conservation. In the north hemisphere, when the fluid column (the height from sea surface to the bottom) is going to be convergent, i.e. a hollow or basin in the sea bed, an anticyclone turning of current could be found in the entire water column body. The same explanation could be used on the other stream curves 'D', 'E', and 'F' in this layer.



(a)



(b)

Fig.11 The Arctic Ocean circulation in the 2nd layers (a) and 1st layer (b), from the Experiment D, The black, blue, green, yellow and red lines are the topography isobath lines of 0m, 1400m, 2000m, 3500m, 4200m.

In the Fig.11-a, the coastal current circulation mostly obey the blue or green isobath

line. The distance between the blue (1,400m) and the green (2,000m) is very small, that means there is a sharp gradient there. This is also an evidence for the potential vorticity conservation. Along the coastal line of the North Greenland Island and Queen Elizabeth and Ellesmere Islands, we could obtain a weak current tightly close to the coastal line, with the direction to the Fram Strait. This is due to the regional reflection by step-like topography. A branch of coastal currents starts to flow to the south, which could be found at the position 'H' in Fig.11-a. And Norwegian-Arctic current also go to the straight from the other side. Fig.12 shows the salinity and temperature structure of Section C, which is selected just across the Fram Strait. It is clear that the relatively colder and saltier Arctic Ocean surface water domains the upper layer of straight, and flows out into the Nordic Sea.

Compared with the present, we lose the signal from atmosphere forcing. That is because the sea ice covers the whole Arctic basin all the time, the heat flux between the ocean and air would be blocked. This ice 'cap' makes the Arctic Ocean more stable and much isolated to the global energy cycle.

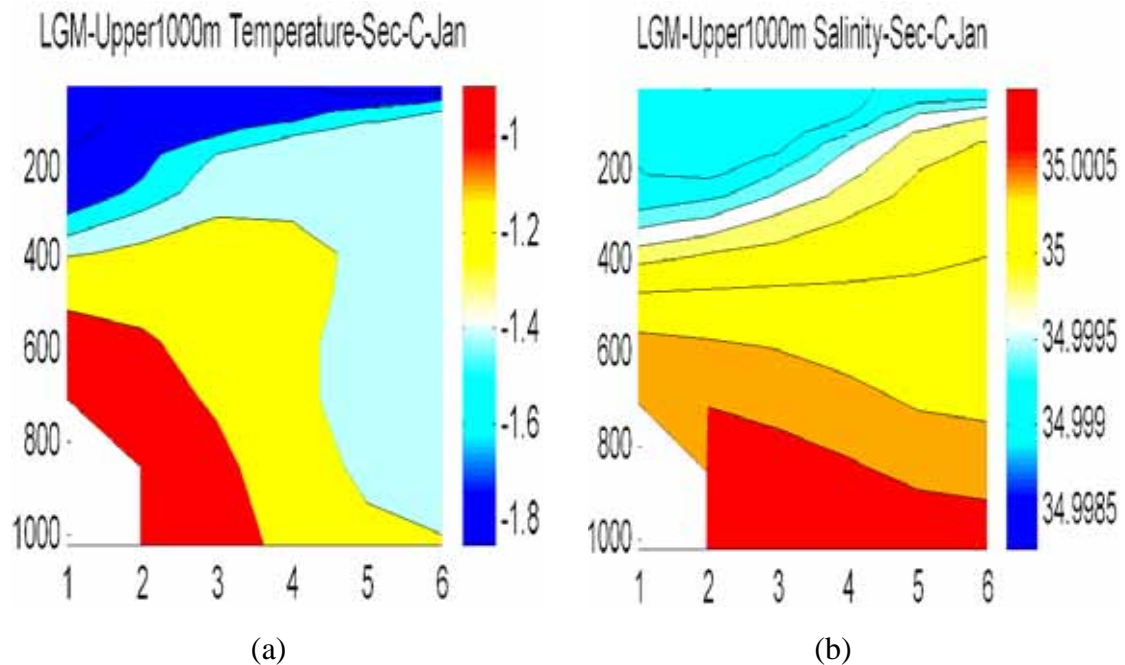


Fig.12 The vertical temperature (a) and salinity (b) section of Section C in the Experiment D.

Step 2

Fig.11-b shows obtained result for Arctic Ocean circulation at the 1st layer within the set up of Experiment D. This pattern includes the information of the basic Arctic Ocean current, which has been discussed in step 1, and the impact from sea ice to the ocean. Compare with the Fig.11-a, the distribution and of current field is almost the same, but the speed of surface ocean water is about 20% lower than the 40m depth in Fig.11-a, that means the friction from the sea ice to ocean consumes 35% kinetic energy of sea surface circulation in Arctic Ocean. Though the sea ice thickness is different from part to part, the effect of sea ice is almost the same everywhere. The ice cap is thick enough to have the ocean to the same constant equilibrium. Along the coastline of Eurasia continent, there is a new coastal current flowing from east to west, the red curve line with an arrow in Fig.11-b. In the bay, at the starting point of the curve, we could only find the inflow at the 40m depth Fig.11-a. We believe that the current in the lower layer into the bay is raised by the continent shelf, and flow back in the upper 20m depth layer. Because the main coastal circulation basically along the 1400m isobath line, and the new found east-west current much more obey the 0m depth coastal line, so there will not too much drag happening, the energy could support it to wonder the entire Eurasia continent coast.

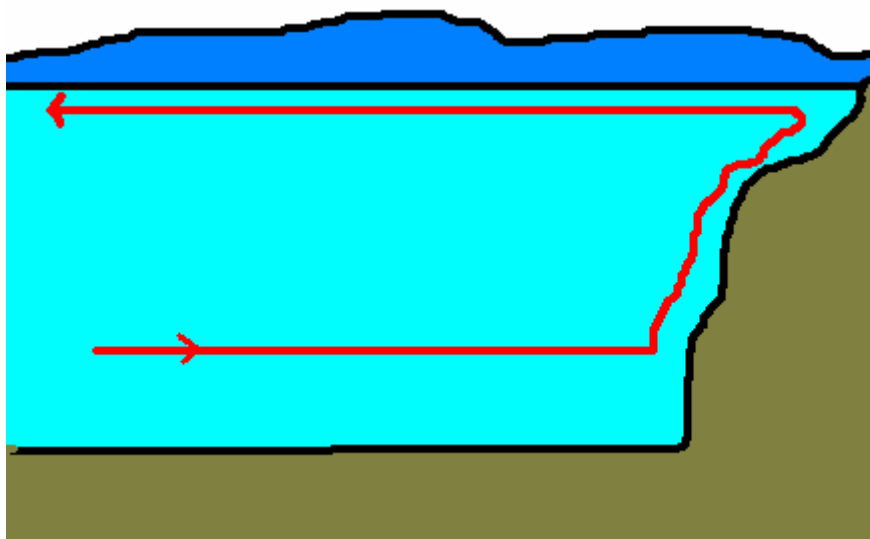


Fig.13 the upwelling currents, cause of the rise of topography in the ‘U’ style bay. The light blue, dark blue and brown mean the sea ice, Arctic Ocean and land.

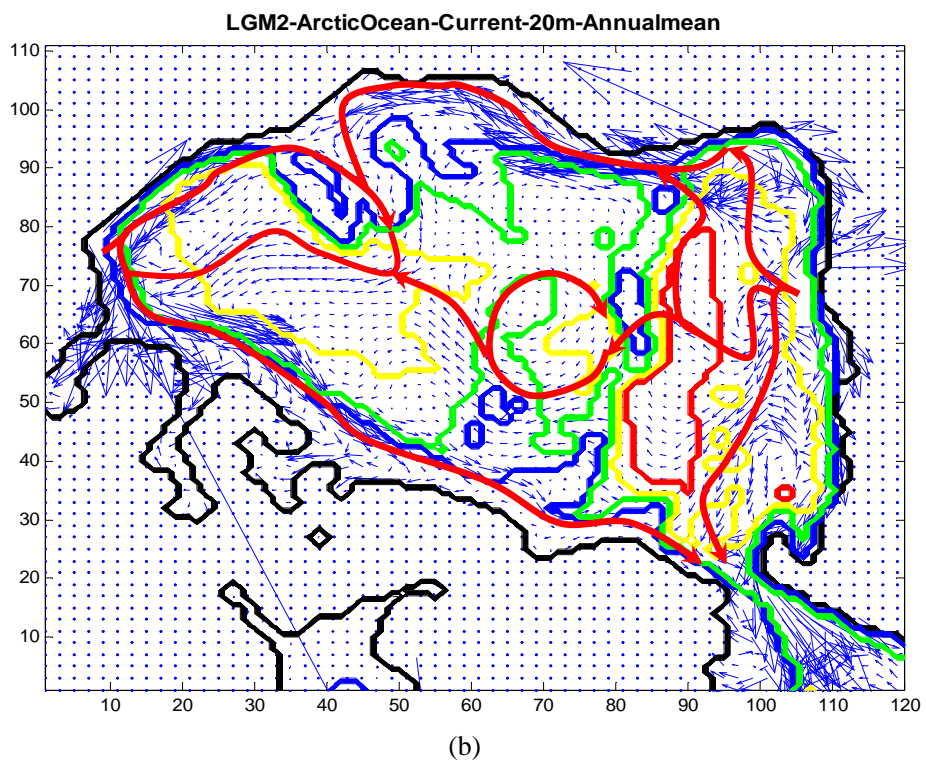
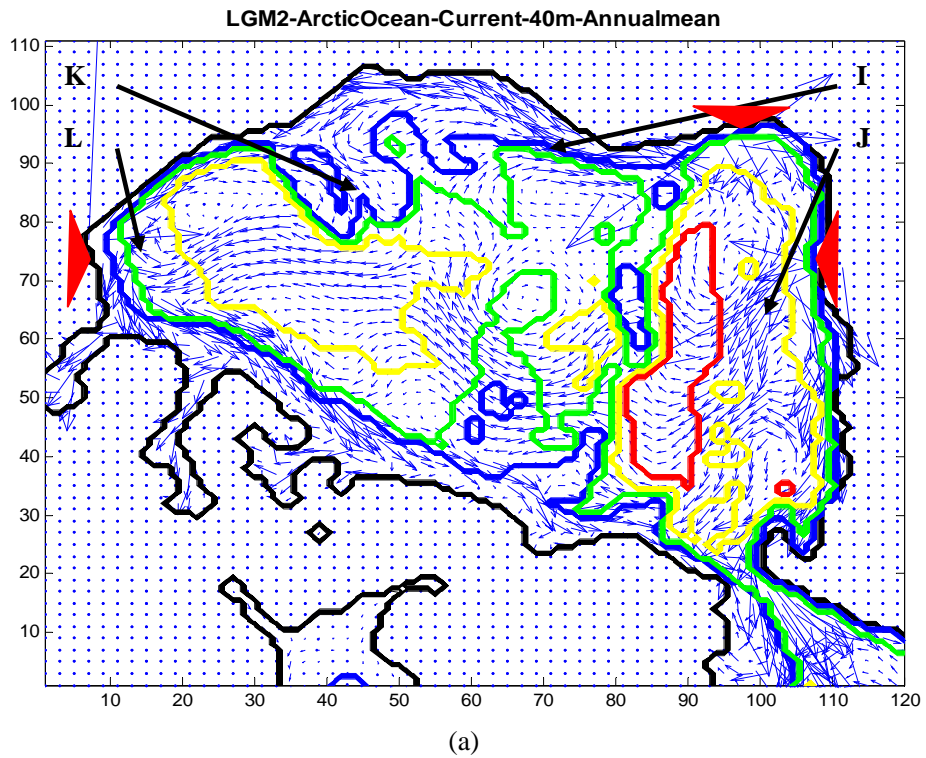


Fig.14 The Arctic Ocean circulation in the 2nd layers (a) and 1st layer (b), from the Experiment E, The black, blue, green, yellow and red lines are the topography isobath lines of 0m, 1,400m, 2,000m, 3,500m, 4,200m.

Step 3

The image of Fig.14-a performs the Arctic Ocean circulation at 40m depth from Experiment E. With the comparison with Fig.11-a, this is the overlay of the river discharge and the basic ocean circulation. The red triangle points the paleo rivers. The fresh water out of the river ports flow along the 0m isobath topography line, the positions 'I' and 'L' show the most obvious difference. Most fresh water from paleo Lena river flows to the west; and most the Eurasia river water join the main basic anticyclone coastal circulation. The paleo Mackenzie River runoff separate into 2 branch: one flows along the Eurasia continent and reach the Chukchi sea; the other currents lies on the North American continent shelf, passing the north boundary of Greenland Island coastline, travels to the Fram Strait. On the surface layer of 'K' position, where is above the Chukchi Sea plateau, the fresh water mass from two continents meet together, then the mixed water turned to the central Arctic Ocean. By potential vorticity conservation, the current turns west above the Canada basin. Due to the injection of paleo Eurasia river, the flow through point 'J', i.e. the 'B' position in the Fig.11-a, increases. But the totally different direction of the basic ocean currents to the fresh discharge on position 'I' would create turbulences and energy lose, the 'S' curve line between the two ocean ridges disappears in the Experiment E.

Step 4

The realistic LGM ocean circulation is showed in Fig.14-b, by red arrowed curves. The influence from sea ice is the same within the Experiment D. Only the current speed gets smaller, but the current field structure never changes. An anticyclone gyre is above the ocean ridge. But the mechanism is totally different from the present Beaufort gyre - not by wind stress, but from vorticity conservation.

The images of Fig.15 visualize the temperature and salinity condition on the Fram Strait in Experiment E. The Arctic Ocean water flow out through the Fram Strait in the surface layer. Due to the mass conservation and stratification, except for the part involved in the thermodynamic process within sea ice and ocean, all the runoff from paleo rivers should flow out of the Arctic Basin in the upper 150m. So the outflow should be greater in the Experiment E. And the sea surface temperature is

-1.75°C, but the river runoff water is nearly 0°C, so it could be regarded as a heat source to the Arctic Ocean. The influence to the salinity by the river should not be considered only locally, because in the dynamics process, ocean circulation makes a bit variation.

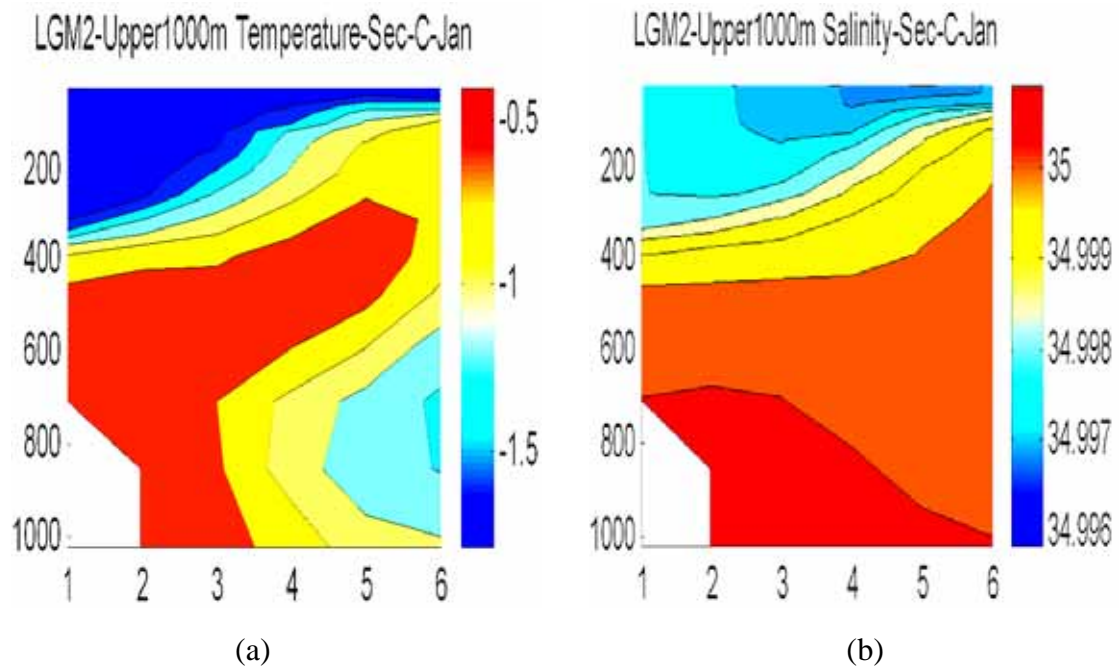


Fig.16 The vertical temperature (a) and salinity (b) section of Section C in the Experiment E.

Step 5

In Experiment F, we set up the model with LGMG atmosphere forcing condition, which offers a relative warmer condition to the model domain area. The image of Fig.16, shows the surface 20m Arctic Ocean currents. Comparing to the 1st layer, ocean circulation is the same. So, the model outcome convince our primary expectation, that the impact to the Arctic Ocean circulation from atmosphere forcing input is very weak or even could be isolated.

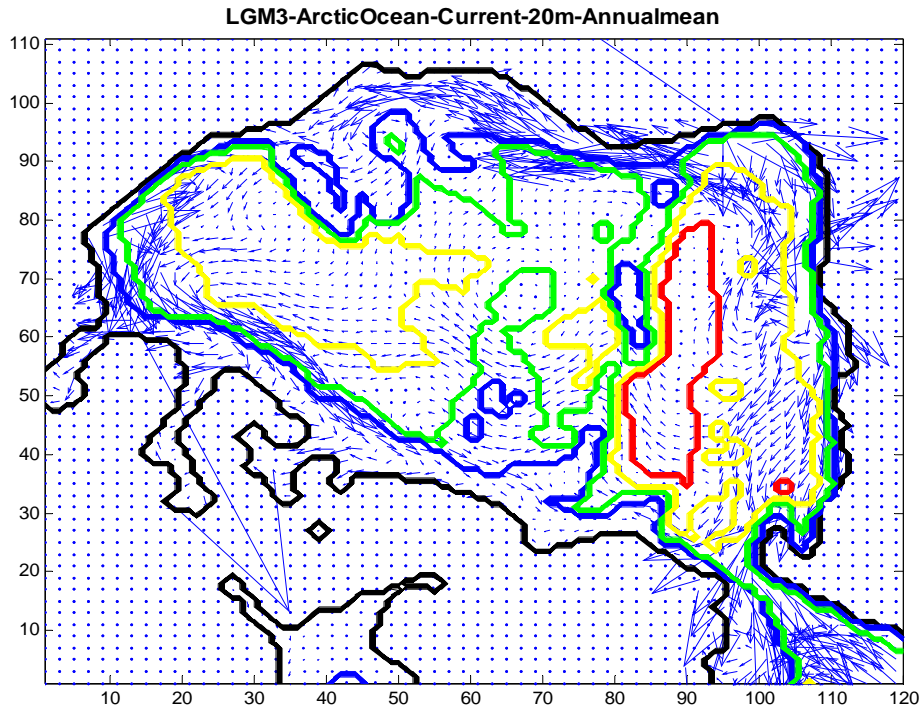


Fig.16 The Arctic Ocean circulation in the 1st layer, from the Experiment F, The black, blue, green, yellow and red lines are the topography isobath lines of 0m, 1400m, 2000m, 3500m, 4200m.

Step 6

In step 6, we will discuss the influence from the North Atlantic Ocean. This is a key factor to the dynamic and thermodynamic process in Arctic Ocean. To eliminate the impact from sea ice, we will choose 40m depth layer.

Fig.17-a is the 2nd upper layer Arctic Ocean circulation with the set up Experiment H. In this assumption, we keep the same amount of stream function at the southern boundary of model domain area, but add 1psu to the salinity and minutes 2 degree for a new thermal forcing. This is a possible estimation to the global mean ocean conditions, and that would increase the density of North Atlantic water, i.e. the kinetic energy. In our primary expectation, this additional energy could support the Atlantic Ocean influence further north.

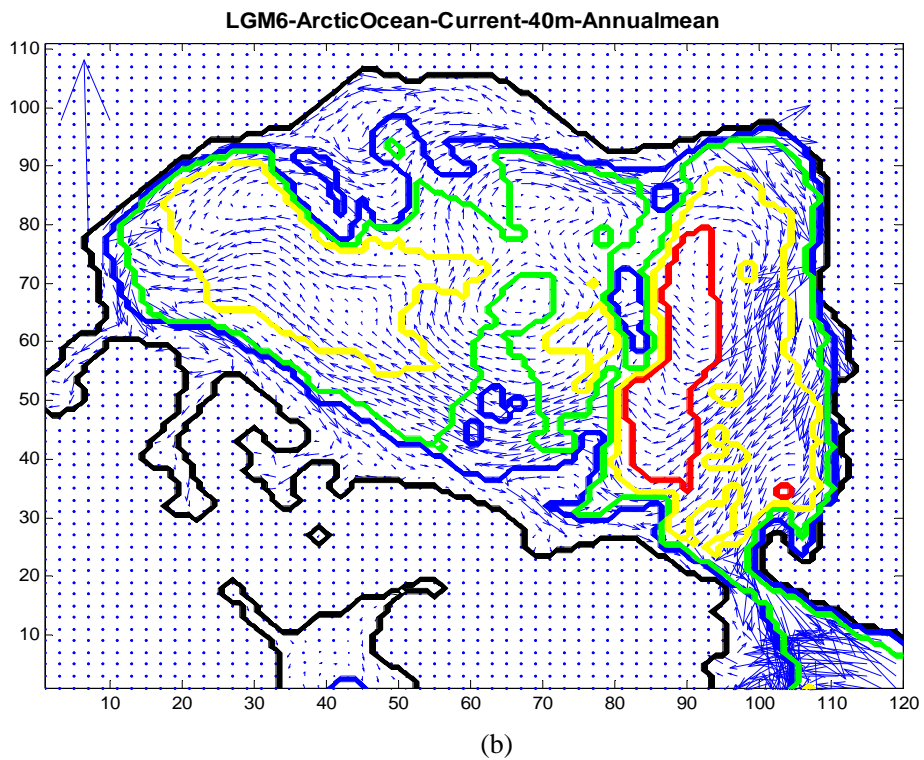
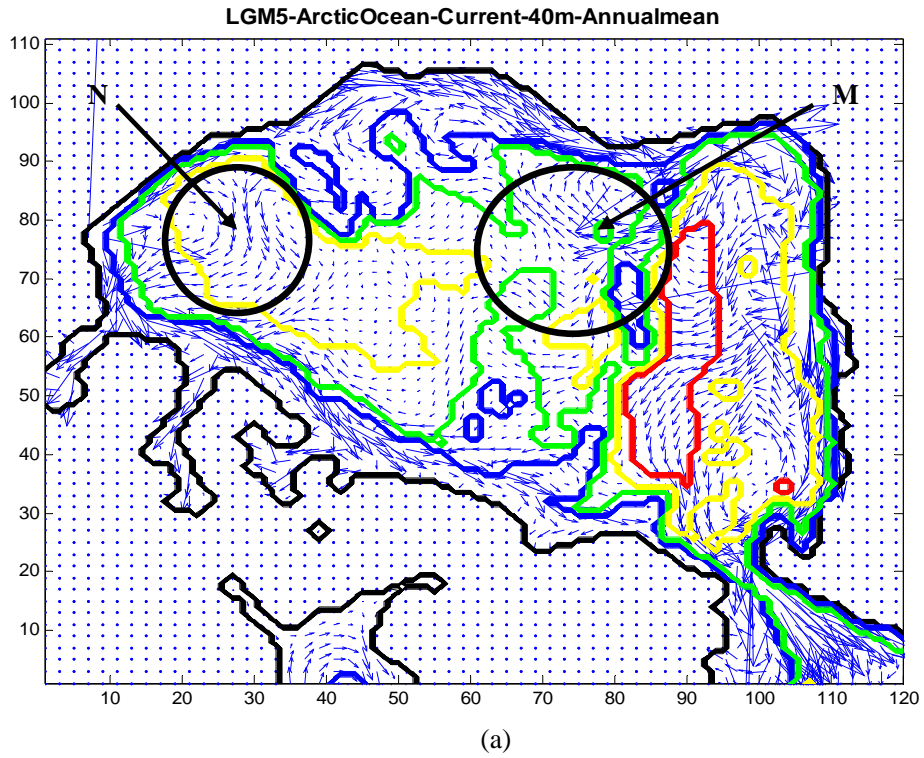


Fig.17 The Arctic Ocean circulation in the 2nd layer, from the Experiment H (a) and I (b), The black, blue, green, yellow and red lines are the topography isobath lines of 0m, 1400m, 2000m, 3500m, 4200m.

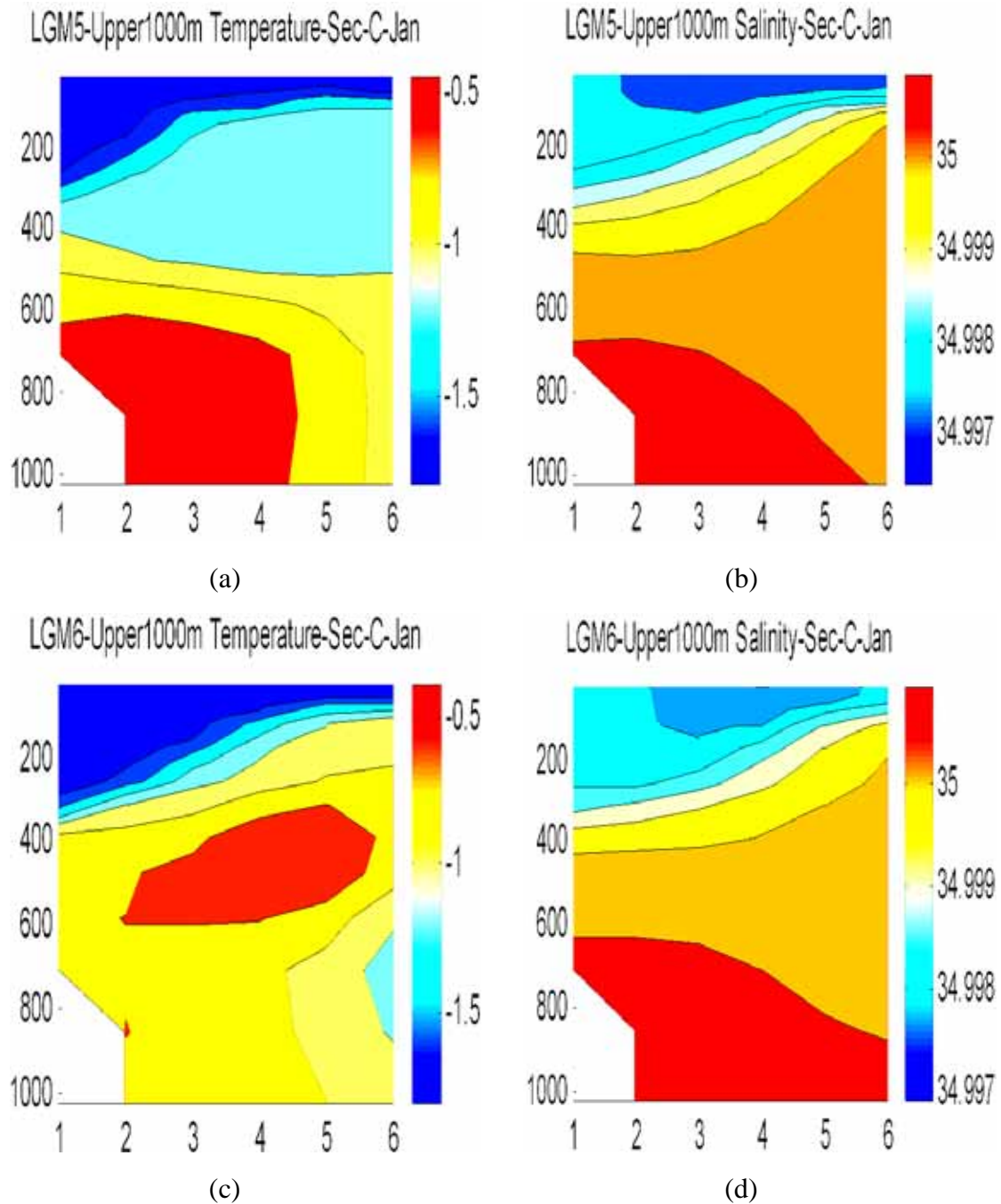


Fig.18 The temperature and salinity structure of Section C in the Experiment H (a, b) and Experiment I (c, d).

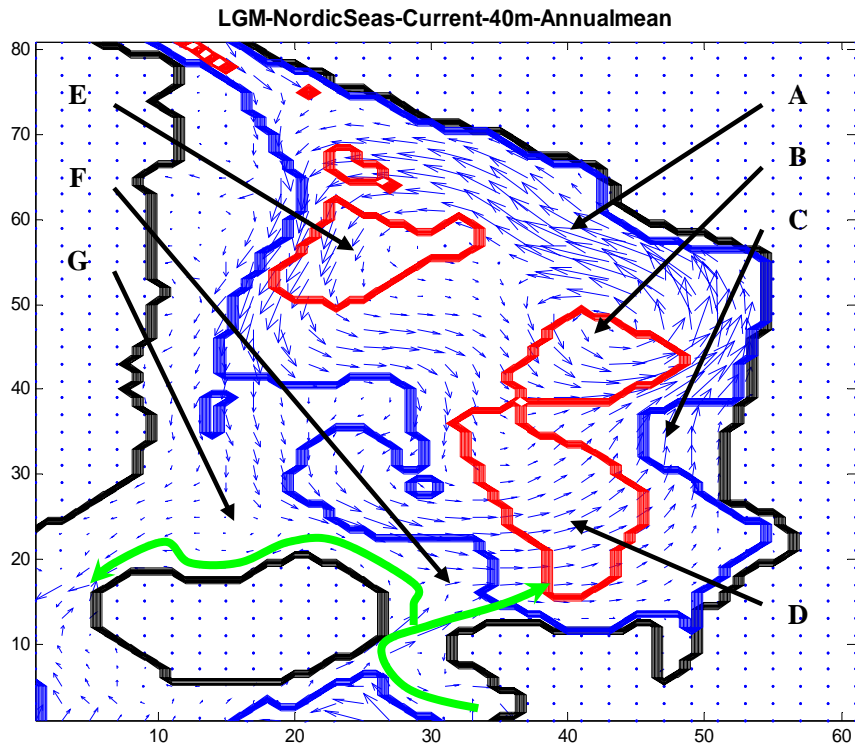
In the image of Fig.17-a, the circulation at the coastal area and the Eurasia basin performs no changes, but in the marked area (Position M & N) it shows a lot or even totally different current features, compared with Experiment E. We can see that, the North Atlantic Ocean water do make sense to the Arctic Ocean circulation, and this could only through the unique channel, the Fram Strait. But we also could see, the

variations are clearly visualized in the very north positions of the Arctic Basin, not the area just north to the entrance. Combined with the temperature and salinity condition of Section C (Fig.18-a & Fig.18-b), we believe the lower latitudes Atlantic Ocean water enters the Arctic basin through the Fram Strait on the subsurface layer (50m – 200m), or also much deeper layers. This current is like an arrow going into the very stable Arctic basin, and it contains sufficient energy to reach the coastal line of Siberian plain. Then the shelf-caused upwelling on position M, as discussed in the Fig.13, brings the water to the surface layer. This path of current breaks the law of potential vorticity conservation.

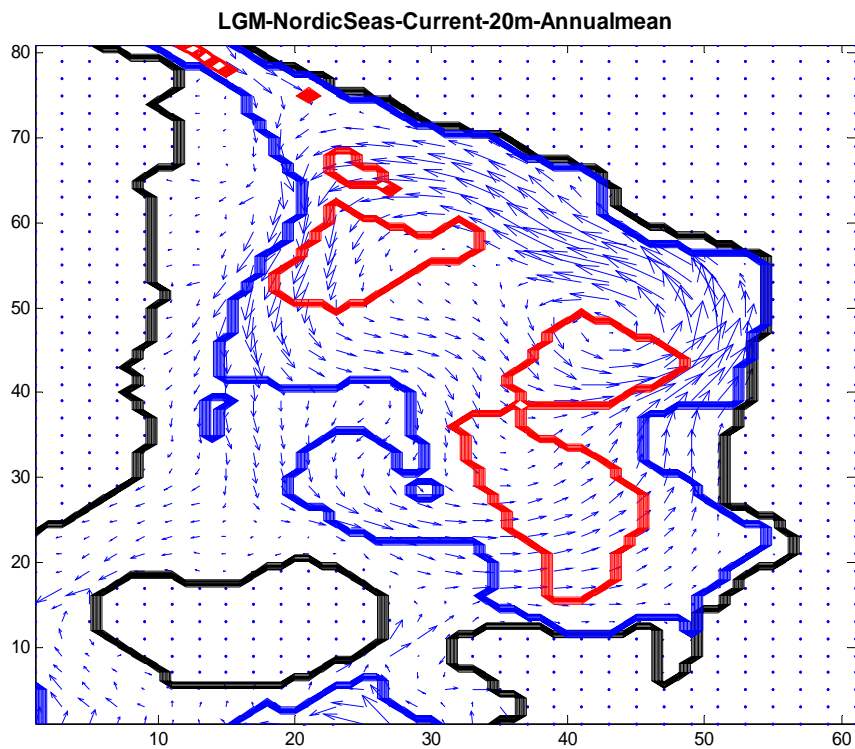
In Experiment I, we assume the ocean boundary stream function to a half. Fig.17-b shows the current field at 40m depth of Arctic Ocean under this set up. In the image, ocean current distribution has the same features with the Fig.14-a. We could see, the sensitivity of North Atlantic Ocean input stream function is not very sensible to the Arctic Ocean surface circulation, at the scale of 50%. The Fig.18 c & d are also very similar to Fig.15 from Experiment E. The loss of stream function has been diminished by the Nordic Seas.

4.1.2 Paleo Nordic Seas Circulation in LGM

Compared with the relatively stable and constant Arctic Ocean, Nordic Sea is much more like a ‘passageway’ area. There are 3 water mass exchange channel: Fram Strait, Denmark Strait and paleo Ice island – Norwegian Strait. The ocean boundary on the Eurasia continent is covered by land ice during LGM, and the Denmark Strait is a bit narrower due to the 120m lower sea surface level. The topography of Nordic seas gets to deeper from west to east, and greater than 4,000m deep ocean basins locate in the south of Fram Strait, and a bit east to the ocean center. In the model set up, the Norwegian land boundary performs not as a continent shelf, but a wall cause of the land ice cover there. To separate the different factors, we would also discuss the Nordic Seas circulation as Tab.2. In Nordic Sea, we analysis the results with a beginning of annual mean, but a seasonal change would also be very necessary.



(a)



(b)

Fig.19 The annual mean Nordic Seas circulation at the 40m depth layer (a) and 20m depth layer (b) of Experiment D. The black, blue and red lines are the topography isobath lines of 0m, 1,400m, and 4,200m.

In the image of Fig.19-a, the ocean current have a anticyclone turning at the position A, B & E; and a cyclone turning at position C. All these could be reasoned by the potential vorticity conservation. The stream line of East Greenland current mostly along the blue topography line; this is cause of the greatest gradient of topography change at about 1,500m depth. In the north of Ice Island (position G), the southwards East Greenland current are separated into 2 branches: one flow further south, through the Davis Strait and will along the continent shelf into the south part of Baffin Bay; the other flow turn to east, and cycle back to the north part of Nordic Sea by the topography forcing. The North Atlantic surface water enters the Nordic Sea only throw the paleo Ice Island-Norwegian Strait, as performed by the green arrow curves. Most low latitudes water will join in the east sub-branch of East Greenland current, and only this part water mass would be transported to the Fram Strait, and influence the Arctic Ocean circulation. A little of Atlantic water, which has successfully through the paleo straight will create a west direction current along the north edge of Ice Island, and flow out of the Nordic Sea.

So, at the surface layer, the Fram Strait and the paleo Ice Island-Norwegian Strait are like entrance, i.e. water mass sources into the Nordic Sea, and the Davis Strait is an exit of ocean current, where water mass are only exported to the south.

Fig.19-b shows the current field at the 1st layer in the Nordic Sea. There are no vast differences comparing with the upper image, and the magnitude of velocity is also very similar. We could say, the sea ice effect in the Nordic Sea is not as strong as in the Arctic Ocean, and it would not be a key factor to influence transporting the North Atlantic Ocean water to the polar region.

We can find the ocean currents in the temperature and salinity section image of Section D in Fig. 20. The current width of west Nordic basin boundary current is a bit wider, but the depth is the same. It is interesting that, a vertically constant region appear just above the sea basin. This could be determined by the distribution of ocean currents, and it changes from time to time, Fig.21.

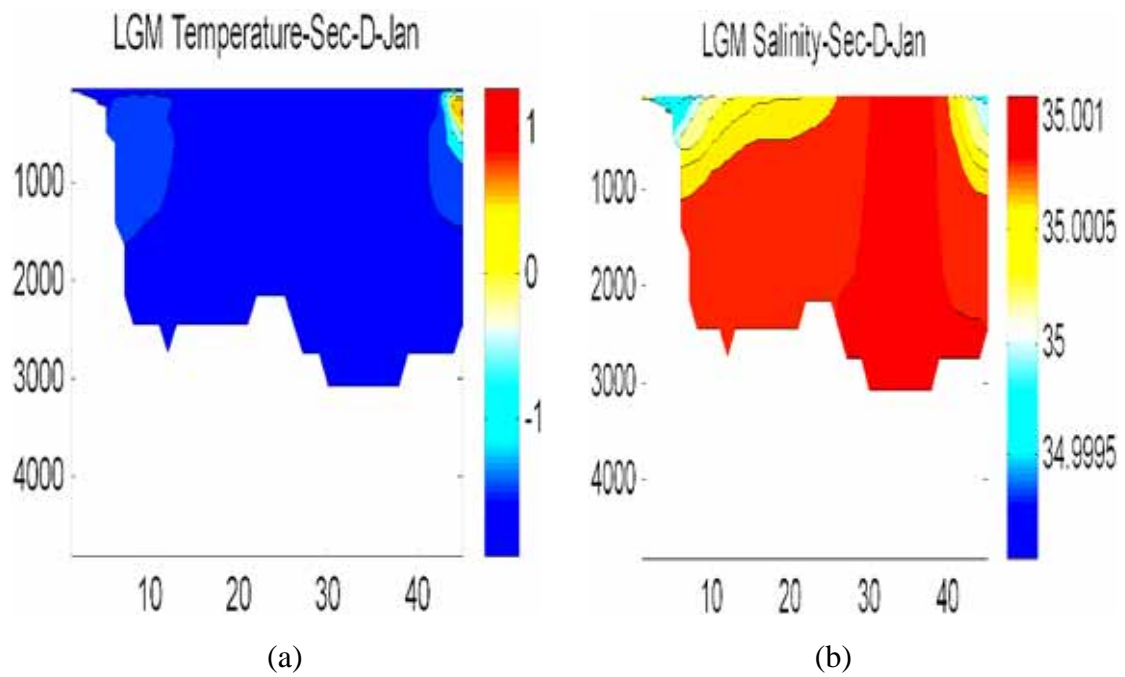


Fig.20 The temperature (Fig.a) and salinity (Fig.b) structure of Section D in the Experiment D.

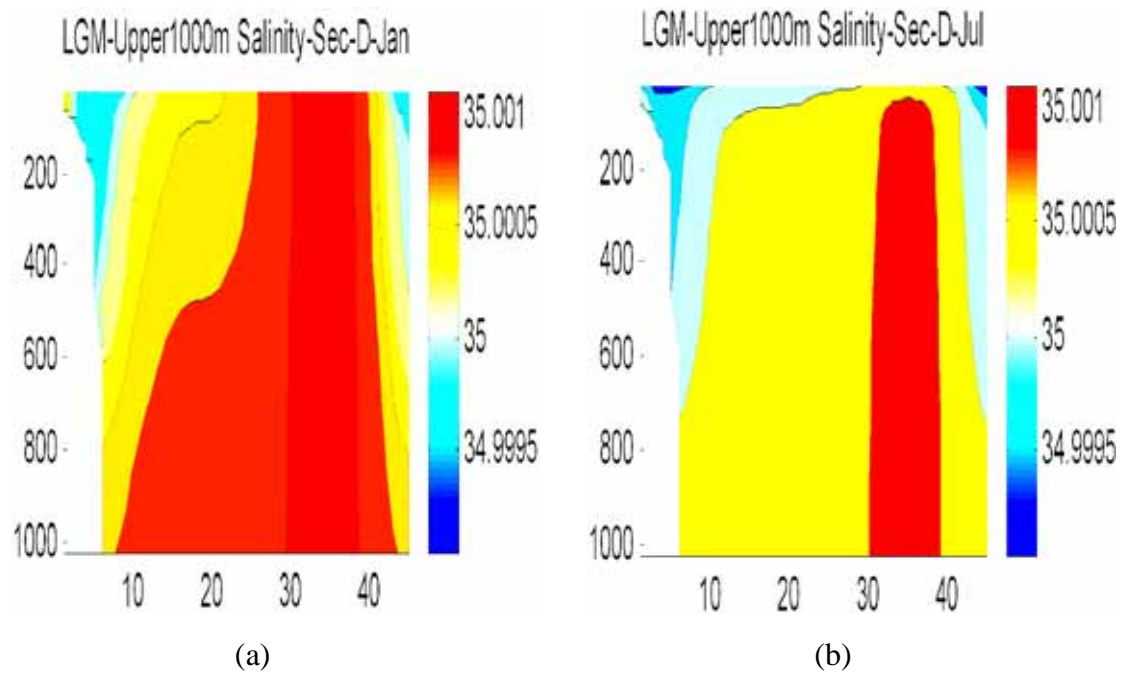


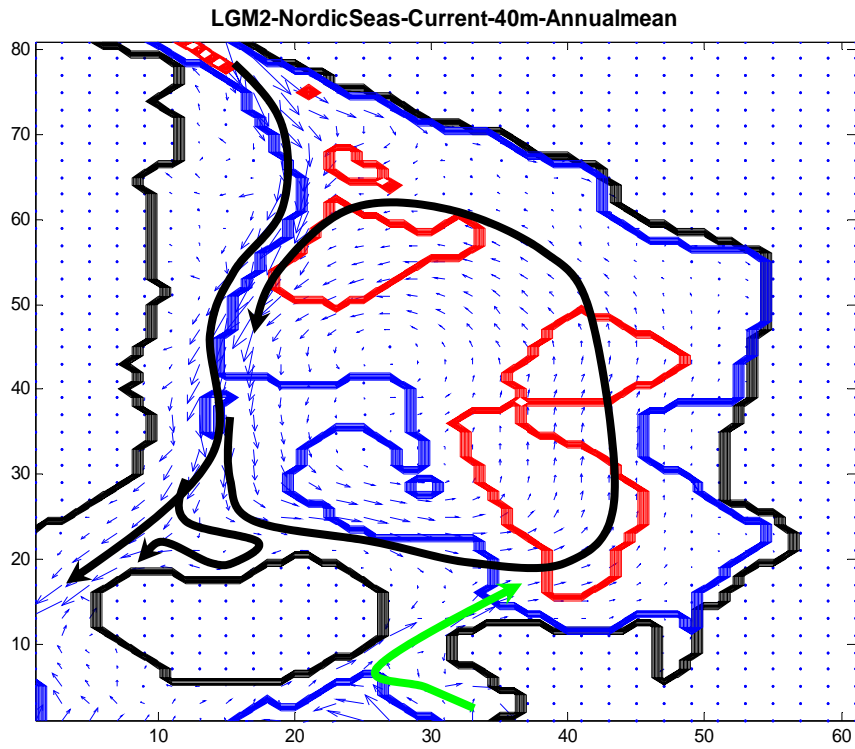
Fig.21 The upper 1000m salinity vertical section in Section D of Experiment D in January (a) and July (b).

In winter (Fig.21-a), the vertical constant reaches the sea surface, and the influence of both eastern and western Nordic Sea boundary currents are isolated from the water

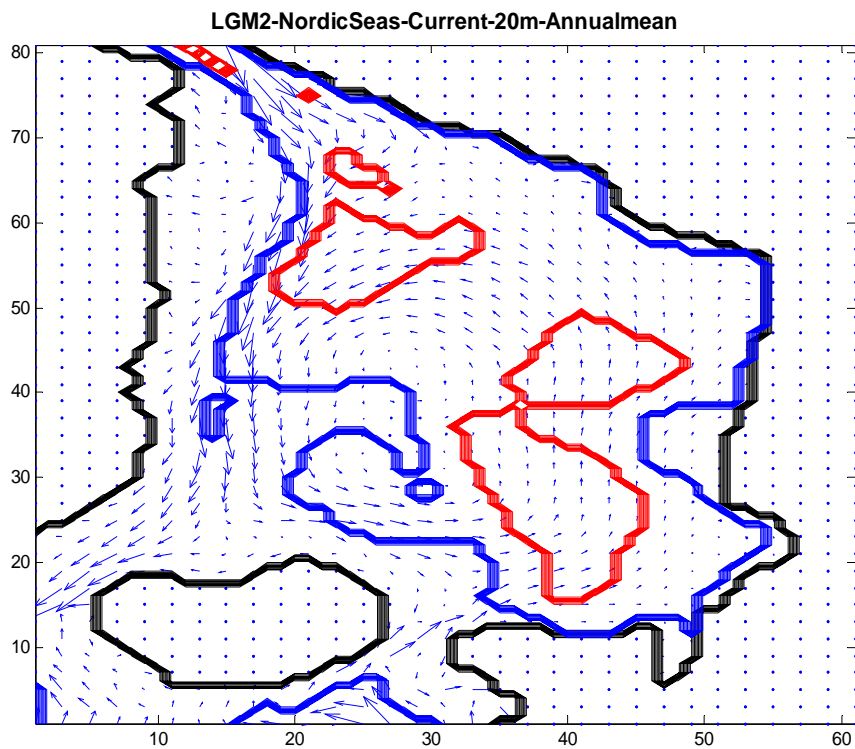
column. But in summer term (Fig.21-b), the upper 50m ocean has been domain by a water mass with relatively lower salinity. Because the perennial constant stratification in Arctic Ocean, it means that there would be more North Atlantic enters Nordic Sea in summer.

The following images of Fig.22 are annual mean Nordic Sea circulation of Experiment E. The upper one belongs to the 40m depth layer, and it is the same with the 20m depth layer (Fig.22-b), but very different to the Fig.18-a. So, the fresh water discharge from paleo Arctic rivers is very important for the surface Nordic Sea currents distribution. Compared with the Experiment D, a ocean basin-scaled cyclone gyre takes the place of the complicated stream curve lines in the image of Fig.19-a, and the Norwegian-Arctic current only locates above the very deep ocean basin, rather than along the 0m isobath line on Eurasia continent. The other very different feature is that, all the lower latitudes water through paleo Ice Island-Norwegian Strait becomes a part of Arctic-Norwegian Current, and is transported to the further north. The similar east-west current along the North Ice Island edge forms by the reflection of topography, not from the North Atlantic Ocean. The message of fresh water discharge in Arctic Ocean could be only delivered through the Fram Strait to the Nordic sea. By the water mass conservation in polar ocean basin, the increased amount of surface outflow equals to the sum of all rivers' runoff. This increase of stream function at the open boundary of Nordic Sea would speed up the water cycle in the ocean basin. In the image of Fig.19-a, the surface circulation describes the ocean topography very well. But in Experiment E, it only shows the mainly bathymetric difference between the Greenland Island shelf and the 4,000m ocean basin. This variation could be referred to the kinetic energy increase of the currents. In other words, the time scale for ocean currents should be long enough to perform the potential vorticity conservation.

In the Fig.23, the images are the section of salinity in Nordic Sea. In July, the 'window' of intermediate layer at the sea surface would be closed by relative less salty and warmer surface water.



(a)



(b)

Fig.22 The annual mean Nordic Seas circulation at the 40m depth layer (a) and 20m depth layer (b) of Experiment E. The black, blue and red lines are the topography isobath lines of 0m, 1,400m, and 4,200m.

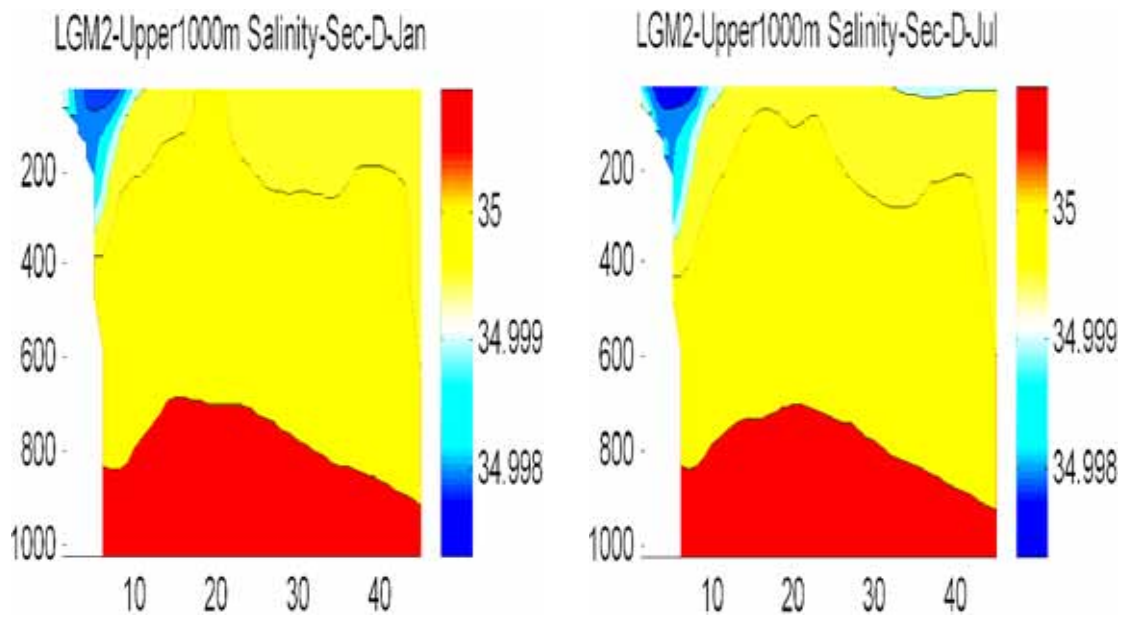


Fig.23 The upper 1000m salinity vertical section in Section D of Experiment E in January (a) and July (b).

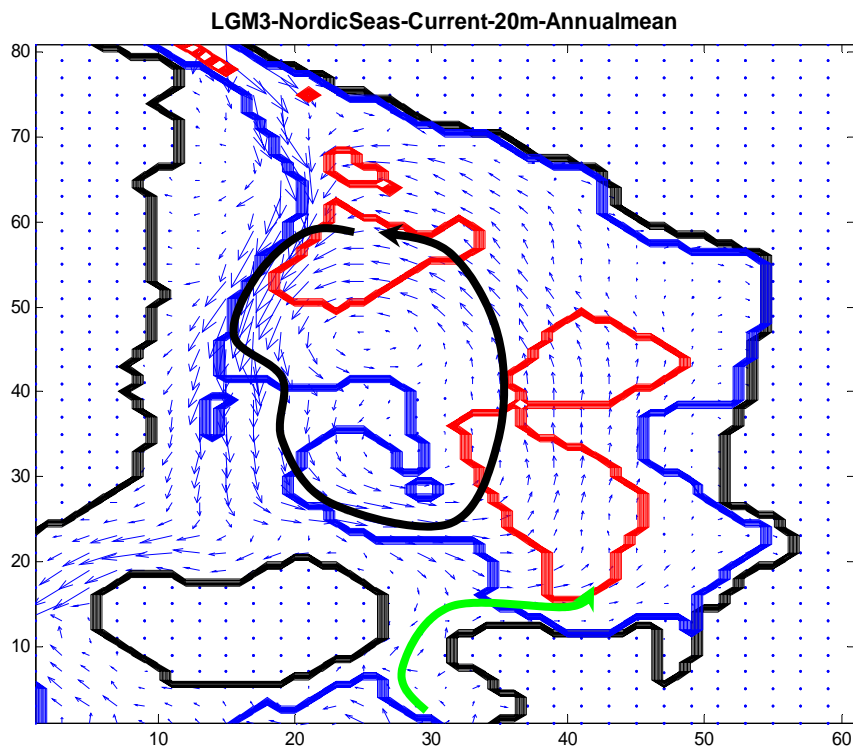
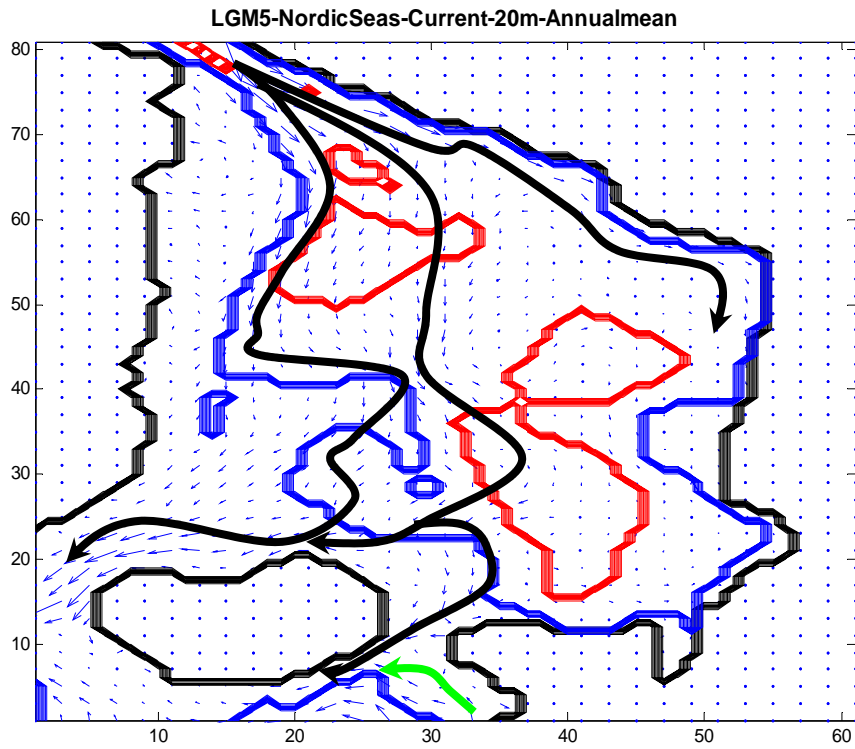


Fig.24 The annual mean Nordic Seas circulation at the 20m depth layer of Experiment F. The black, blue and red lines are the topography isobath lines of 0m, 1,400m, and 4,200m.

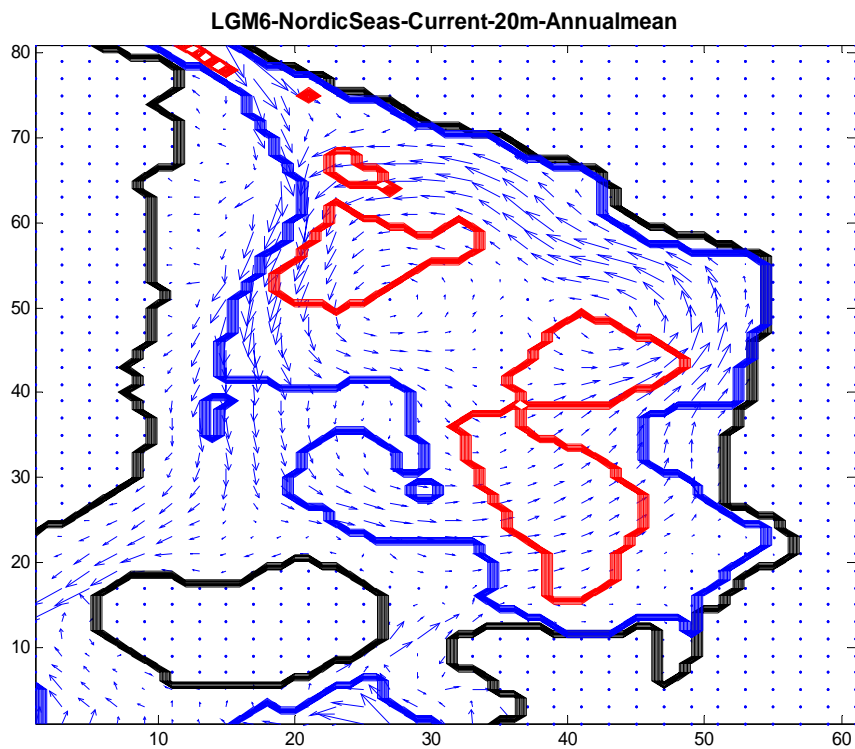
In Experiment F, we set up the model with LGMG atmosphere forcing condition, which offers a relative warmer condition to the model domain area. The image of Fig.24 shows the Nordic Sea currents in the surface 20m layer, simulated in Experiment F. It has the basically same circulation. So, the Nordic Sea surface circulation is mostly independent to the atmosphere variation.

The image of Fig.25-a performs the Nordic Seas surface circulation of Experiment H. When the North Atlantic surface water gets to much saltier and colder, the currents shows a totally different status. The Arctic Ocean outflow separates to 3 sub-currents: one branch passes through the central Nordic Seas; while the other 2 flows travel along the west and east 1,400m isobath line to the south. The most important is the water budget changes at the paleo Ice Island – Norwegian Strait. It becomes a pure exit of Nordic Seas surface layer water. So within the Experiment H set up, the Nordic Seas would not influenced by the North Atlantic surface water. And as the performance of 40m depth Arctic Ocean circulation in Fig.17-a image, there would be a subsurface Atlantic Ocean current entering the Arctic Ocean through the vertically constant column above the 4000m Nordic Seas basins, and reaches the coastal area of East Siberian Sea.

In Fig.17-b, a half discount of ocean boundary stream function doesn't make change to the surface Arctic Ocean circulation. But this change shows a new current distribution in the Nordic Seas, as performed in Fig.25-b. The type of Nordic Seas circulation in Experiment I is much more like the outcomes from the set up of Experiment D, in Fig.19-b. In other words, the influence caused by a reduction of stream function at ocean boundary is similar to the miss of the fresh water discharge. As argued above, this due to the ocean current vorticity has the same magnitude with the planet vorticity. The ocean topography rules the circulation very well.



(a)



(b)

Fig.25 The Nordic Sea surface circulation in the 1st layer, from the Experiment H (a) and I (b), The black, blue, and red lines are the topography isobath lines of 0m, 1400m, and 4200m

4.2 Sea Ice Distribution and Transport

The realistic LGM sea ice cover is shown in Fig.26. The Arctic Ocean is covered by perennial sea ice. The multiyear annual mean value of ice thickness is about 12m. Some thickest points are in the small bays near the Queen Elizabeth Islands, which is 25m thick. From the thickness distribution, we could see the influence of fresh water to the ice formation. In LGM, the river discharge is about 0 degree. But it is still relatively warmer than the Arctic Ocean surface water, so it could be regarded as heat sources. In Fig.26-a & b, the green, blue regions are along the coastal line, and extend to the central Arctic Ocean above the Chukchi ocean plateau, which is quite similar to the sea surface salinity distribution. At the river port of paleo Mackenzie River, the sea ice is only 2m-4m thick.

Arctic Ocean sea ice concentration is stable and constant almost everywhere. The ice is drifted by the outflows through Fram Strait to the Nordic Seas, Fig.27. The big cyclone circulation gyre bring warm North Atlantic Ocean water to the north part of Nordic Seas, so the great gradient of sea ice change could be see at the Fram Strait. The average of Nordic sea ice is about 6m thick, and along the Barents land ice sheets, the thickness there could be less than 2m. On the western edge of Nordic Sea, the East Greenland current transports sea ice to the Davis Strait, and then they are blocked by Ice Island. Part of ice is drifted further south to the Labrador Sea by a eastern branch of the East Greenland current; and the left would meet the warm Atlantic water, which has successfully passed through the paleo Ice Island - Norwegian Strait. We can clearly see the sea ice drift from the ice concentration performance in Fig.27-c & d. Sea ice was drifted to the Fram Strait by the Arctic Ocean surface outflows. In winter, with cooperation of the northwards wind and southwards ocean current, there would be complete ice concentration and high thickness on the channel. This growth process of sea ice there could be observed from October to next June. In summer, the wind rotated to southwards, i.e. the ocean and atmosphere make the positive contribution to sea ice exporting from Arctic Ocean. The ice, covering the straight, brakes and are transported into the Nordic Seas by Paleo East Greenland Current.

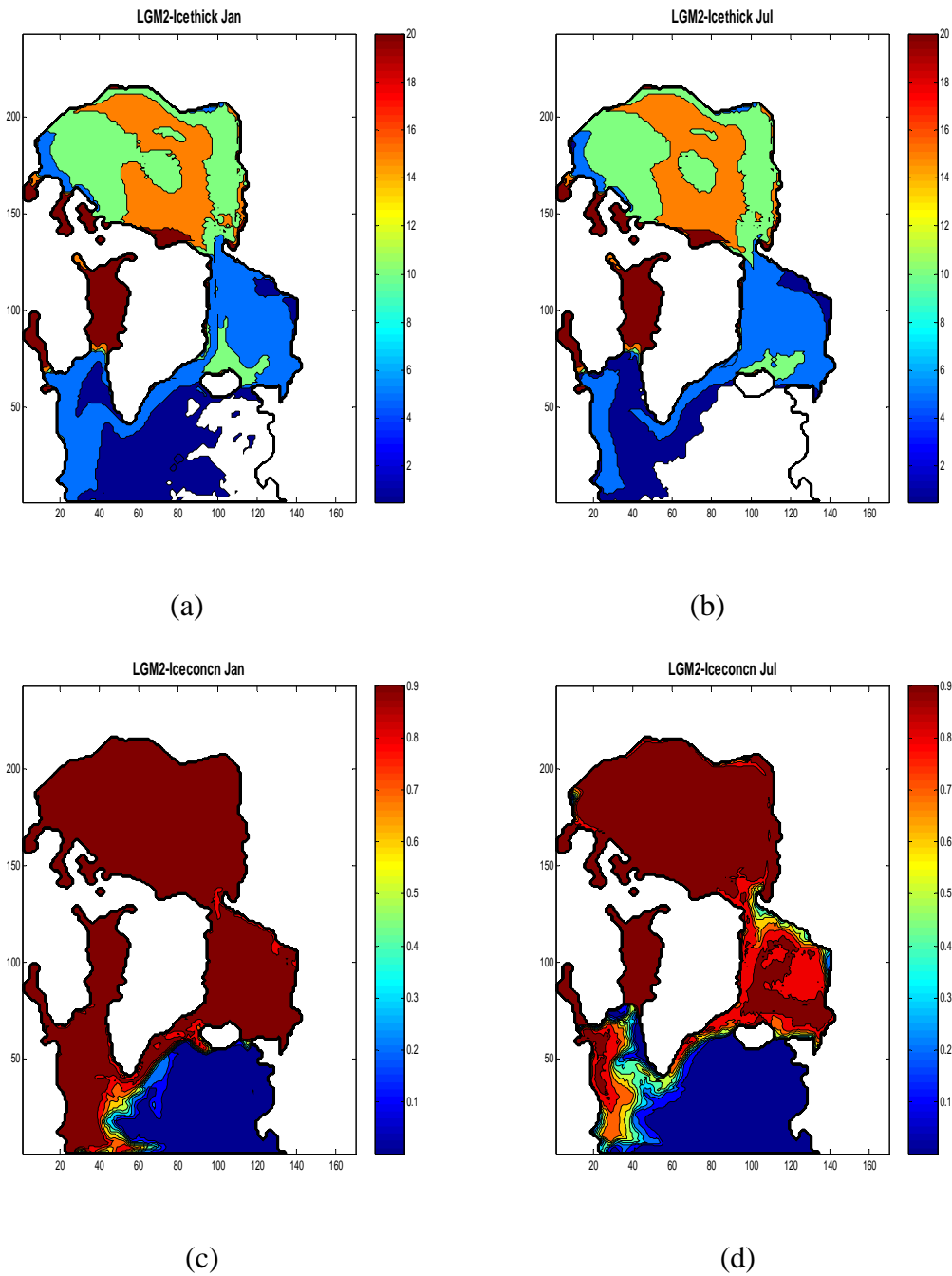


Fig.26 Images a & b are the sea ice thickness of the realistic LGM run (Experiment E) in January and July, and the lower figures c & d perform the sea ice concentration. The white part in the North Atlantic Ocean area of image a and b, indicate where free of sea ice cover.

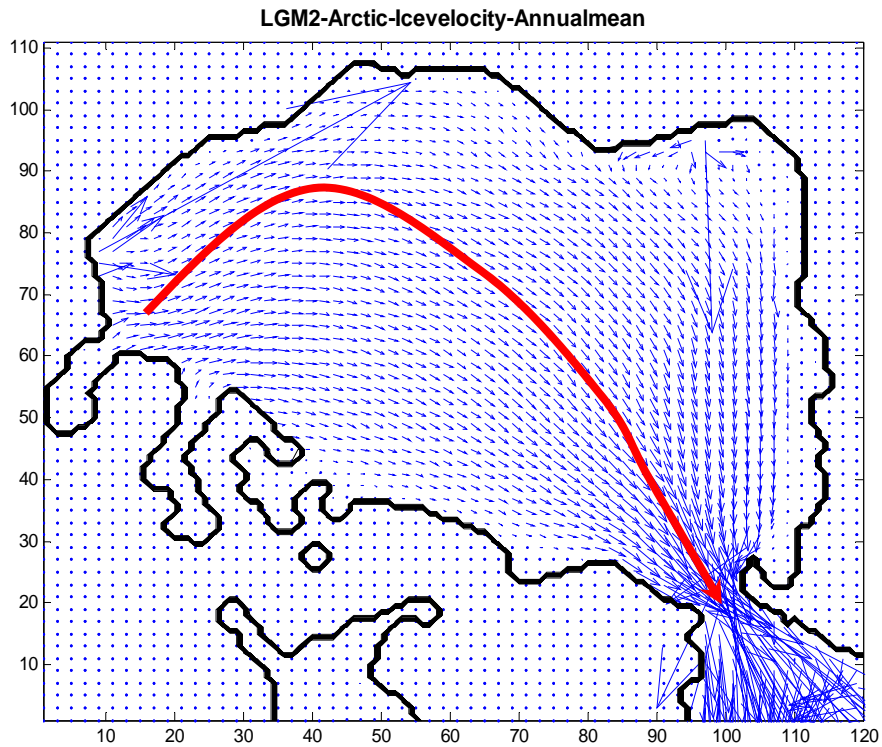


Fig.27 Multi-year annual mean of ice drift velocity in Arctic Ocean, from the Experiment E.

The average temperature in the bottom layer of atmosphere in LGM summer is about -20°C around the North-east Greenland ocean areas. Such a cold condition has the local sea ice formation immediately in the sea ice-broken areas. So, there are obvious ice concentration variation and ice break in Fram Strait during summer term in LGM, but there might be no ice-free open area due to this cold atmosphere conditions. In the west part of Nordic Seas, where the Paleo East Greenland Current exists, the Arctic sea ice is transported by the southwards flows through Fram Strait. The ice concentration is greater than 0.8, and nearly to 1 in most time of year, because of a huge amount flake ice drifted there all the time. The center in the Nordic sea is domain by the nearly constant deep Nordic water mass, which contains more salt, and higher temperature than the surface water mass. So, sea ice in the central Nordic Seas is not as strong as the eastern part of Nordic Sea, and strong cyclone ocean circulation and seasonally changing wind stress could tear sea ice much easier. The ice

concentration is only 0.6 in summer, some paleo evidences, e.g. sediment cores, were available in this area. The warmer Norwegian-Arctic current could weaken the sea ice in the region along the Barents Sea land ice edge, and the katabatic wind from hundreds meters height ice sheet mountains could enlarge and hence the cracks and flaws of sea ice. That is how the open area forms on the east boundary of Nordic Sea. And this process gives the possibility of Barents Sea land ice expansion from the beginning of last glacial period to LGM.

5. Conclusions

6. Bibliography

- [1] Michael Pidwirny (2006) *Introduction to the Oceans*
- [2] Swift, J.H., Jones, E.P., Aagaard, K., Carmack, E.C., Hingston, M., Macdonald, R.W., McLaughlin, F.A., and Perkin, R.G. (1997) *Waters of the Makarov and Canada basins, Deep-Sea Research, 44, 1503-1530*
- [3] Carmack, E.C. Aagaard, K., J.H., Perkin, R.G., McLaughlin, F.A., Macdonald, R.W., Jones, E.P., Smith, J.Ellis, K., And Kilius, L. (1997) *Change in temperature and tracer distributions within the Arctic Ocean: Results from the 1994 Arctic Ocean section, Deep-Sea Research, 44, 1487-1502*
- [4] Sidney Draggan, etc. (2008) *State of Arctic report (National Oceanic and Atmospheric Administration)*
- [5] Edward Lyn Lewis, E.Peter Jones, Peter Lemke, Terry D. Prowse and Peter Wadhams (1998) *The Freshwater Budget of the Arctic Ocean*
- [6] Milliman, J.D. and Meade, R.H. (1983) *World-wide delivery of river sediment to the oceans, Journal of Geology, 91, 1-21, 1983*
- [7] Stigebrandt, A. (1981) *A model for the thickness and salinity of the upper layer in the Arctic Ocean and the relationship between the ice thickness and some external parameters, Journal of Physical Oceanography, 11, 1407-1422.*
- [8] Bjoerk, G. (1989) *A one-dimensional time-dependent model for the vertical stratification of the upper Arctic Ocean, Journal of Physical Oceanography, 19,*

52-67.

[9] J. Richter-Menge¹, J. Comiso², W. Meier³, S. Nghiem⁴, and D. Perovich¹ (2008), *Sea Ice Cover*

[10] Chapman, W.L., and J.E. Walsh, 2007: *Simulations of Arctic temperature and pressure by global coupled models. J. Climate*, 20, 609–632.

[11] J. Richter-Menge, J. Overland, et al (2008), *Arctic Report Card 2008*

[12] Swift, J.H. and Aagaard, K.(1981) *Seasonal transitions and water mass formation in the Iceland and Greenland seas, Deep-Sea Research*, 28, 1107-1129

[13] Aagaard, K. And Carmack, E.C. (1994) *The Arctic and climate: A perspective, in The Polar Oceans and Their Role in Shaping the Global Environment, in O.M. Johannessen, R.D. Muench and J.E. Overland (eds.), Geophysical Monograph Series*, 85, AGU, Washington, D.C., pp. 4-20

[14] Thomas Schneider, Andrey Ganopolski, Hermann Held, Stefan Rahmstorf (2006) *How cold was the Last Glacial Maximum?*

[15] Moeller, P. et al. *Severnaya Zemlya, Arctic Russia: a nucleation area for Kara Sea ice sheets during the Middle to Late Quaternary, Quaternary Science Review Vol. 25, No. 21-22, pp. 2894-2936, 2006.*

[16] Matti Saarnisto, *Climate variability during the last interglacial-glacial cycle in NW Eurasia. Abstracts of PAGES-PEPIII: Past Climate Variability Through Europe and Africa, 2001*

[17] Lyn Gaultieri et al. *Pleistocene raised marine deposits on Wrangel Island, northeast Siberia and implications for the presence of an East Siberian ice sheet, Quaternary Research, Vol. 59, NO.3, pp. 399-410, May 2003.*

[18] Zamoruyev, V., 2004, *Quaternary glaciations of north-east Asia. Quaternary Glaciations: Extent and Chronology: Part III: South America, Asia, Africa, Australia, Antarctica, pp 321-323*

[19] 物理海洋

[20] 海冰 1979

[21] Gerdes, R., M. Karcher, F. Kauker, and C. Koeberle, *Predicting the spread of radioactive substances from the Kursk, Eos. Trans. AGU*, 82,253,256-257, 2001.

- [22] Karcher, M., R. Gerdes, F.Kauker, and C. Koeberle, *Arctic warming: Evolution and Spreading of the 1990s warm event in the Nordic Seas and the Arctic Ocean*, *J. Geophys. Res.*, 108(C2), 3034, doi: 10.1029/2001JC001265, 2002.
- [23] Pacanowski, R. C., *MOM 2 Documentation, user's guide and reference manual*, GFDL Ocean Group Tech. Rep.3, Geophys. Fluid Dyn. Lab., Princeton Univ., Princeton, N.J., 1995.
- [24] Zalesak, S. T., *Fully multidimensional flux-corrected transport algorithms for fluids*, *J. Comput. Phys.*, 31, 335-362, 1979.
- [25] Gerdes, R., C. Koeberle, and J. Willebrand, *The influence of numerical advection schemes on the results of ocean general circulation models*, *Clim. Dyn.*, 5, 211-226, 1991.
- [26] Koeberle, C., and R. Gerdes, *Mechanisms determining variability of arctic ice conditions and export*, *J. Clim.*, 2003.
- [27] Hibler, W. D., *A dynamic thermodynamic sea ice model*, *J. Phys. Oceanogr.*, 9, 815-846, 1979.
- [28] Harder, M., P. Lemke, and M. Hilmer, *Simulation of sea ice transport through Fram Strait: Natural variability and sensitivity to forcing*, *J. Geophys. Res.*, 103, 5595-5606, 1998.
- [29] Semtner, B., *A model for the thermodynamic growth of sea ice in numerical investigations of climate*, *J. Phys. Oceanogr.*, 379-389, 1976.
- [30] Kauker, F., Gerdes, R., Karcher, M., Koeberle, C., and Lieser, J.L., *Variability of Arctic and North Atlantic sea ice: A combined analysis of model results and observations from 1978 to 2001*, *J. Geophys. Res.*, 108(C6), 3182, doi: 10.1029/2002JC001573, 2003.
- [31] Stevens, D. P., *The open boundary condition in the United Kingdom Fine-Resolution Antarctic Model*, *J. Phys. Oceanogr.* 21, 1494-1499, 1991.
- [32] Levitus, S. R. Burgett, and T. Boyer, *World Ocean Atlas 1994, vol. 3, Salinity*, NOAA Atlas NESDIS, vol. 4, Natl. Oceanic and Atmos. Admin. Silver Spring, Md., 1994.
- [33] Levitus, S., R. Burgett, and T. Boyer, *World Ocean Atlas 1994, vol. 3, Salinity*,

NOAA Atlas NESDIS, vol. 3, Natl. Oceanic and Atmos. Admin. Silver Spring, Md., 1994.

[34] National Snow and Ice Data Center (NSIDC), *Joint U.S. Russian Atlas of the Arctic Ocean, Oceanography Atlas for the Winter Period [CD-ROM]*, Environ. Working Group, Univ. of Colo., Boulder, 1997.

[35] Kalnay, E., et al., *The NCEP/NCAR 40-Year Reanalysis Project*, Bull. Am. Meteorol. Soc., 77, 437-495, 1996.

[36] Clark, P. U., Mix, A. C., *Ice sheets and sea level of the Last Glacial Maximum*, Quaternary Science Reviews 21,1-7, 2002.

[37] Svendsen, J.I., et al., *Late Quaternary ice sheet history of northern Eurasia*, Quaternary Science Reviews 23,1229-1271, 2004.

[38] Clark, P. U., Alley, R. B., Pollard, D., *Northern Hemisphere Ice-Sheet Influences on Global Climate Change*, Science, vol.286 (11), 1999.

[39] Svendsen, J.I., et al., *Maximum extent of the Eurasia ice sheets in the Barents and Kara Sea region during the Weichselian*, Boreas, 28(1), 234-242, 1999.

[40] Dyke, A. S., J. T. Andrews, Clark, P. U., et al., *The Laurentide and Innuitian ice sheets during the Last Glacial Maximum*, Quat. Sci. Rev, 21, 9-31, 2002.

[41] England, J., *Coalescent Greenland and Innuitian ice during the Last Glacial Maximum: Revising the Quaternary of the Canadian High Arctic*, Quat. Sci. Rev., 18(3), 421-456, 1999.

[42] Vogt, C., Knies, J., *Sediment dynamics in the Eurasian Arctic Ocean during the last deglaciation – The clay mineral group smectite perspective*, Marine Geology, 250: 211-222, 2008

[43] Alkama, R., Kageyama, M., et al., *Impact of a realistic river routine in coupled ocean-atmosphere simulations of the Last Glacial Maximum climate*, Climate Dynamics, 30: 855-869, doi: 10.1007/s00382-007-0330-1, 2008

[44] Alkama, R., Kageyama, M., Ramstein, G., *Freshwater discharges in a simulation of the Last Glacial Maximum climate using improved river routing*, Geophysical Research Letter, vol.33, L 21709, doi: 10.1029/2006GL027746,2006

[45] Marshall, S. J., Clarke, G. K., *Modeling North American Freshwater Runoff*

- through the Last Glacial Cycle, Quaternary Research, 52: 300-315, 1999*
- [46] Roeckner E., Arpe K., Bengtsson L., et al., *Simulation of the presentday climate with ECHAM model: impact of model physics and resolution, S. 28, Hamburg, Germany, pp171, 1992.*
- [47] Lohmann, G., Lorenz, S., *On the hydrological cycle under paleoclimatic conditions as derived from AGCM simulations, Journal of geophysical research, vol.105, D13: 17417-17436, 2000*
- [48] Romanova, V., Prange, M., Lohmann, and G., *Stability of the glacial thermohaline circulation and its dependence on the background hydrological cycle, Climate Dynamics 22:527-538, doi: 10.1007/s00382-004-0395-z, 2004.*
- [49] CLIMAP Project Members, *The surface of the Ice-Age Earth, Science, 191, 1131 – 1137,1976.*
- [50] CLIMAP Project Members, *Seasonal reconstructions of the Earth's surface at the Last Glacial Maximum, Geol. Soc. of Am. Map and Chart Ser., MC-36, Geol Soc. Of Am., Boulder, Colo., 1981.*
- [51] Hebbeln, D., T. Dokken, E. S. Andersen, M. Hald, and A. Elverhøi, *Moisture supply for northern ice-sheet growth during the Last Glacial Maximum, Nature, 370, 357– 360, 1994.*
- [52] Sarnthein, M., et al., *Variations in Atlantic surface ocean paleoceanography, 50o–800N: A time-slice record of the last 30,000 years, Paleoceanography, 10(6), 1063– 1094, 1995.*
- [53] Weinelt, M., M. Sarnthein, U. Pflaumann, H. Schulz, S. Jung, and H. Erlenkeuser, *Ice-free Nordic Seas during the Last Glacial Maximum? Potential sites of deepwater formation, Paleoclimatology, 1, 283– 309, 1996.*
- [54] Sarnthein, M., R. Gersonde, S. Niebler, U. Pflaumann, R. Spielhagen, J. Thiede, G. Wefer, and W. Weinelt, *Overview of Glacial Atlantic Ocean Mapping (GLAMAP 2000), Paleoceanography, 18(2), 1030, doi:10.1029/2002PA000769, 2003a.*
- [55] Sarnthein, M., U. Pflaumann, and M. Weinelt, *Past extent of sea ice in the northern North Atlantic inferred from foraminiferal paleotemperature estimates, Paleoceanography, 18(2), 1047, doi:10.1029/2002PA000771, 2003b.*

- [56] Rosell-Mele, A., and N. Koc., *Paleoclimatic significance of the stratigraphic occurrence of photosynthetic biomarker pigments in the Nordic Seas*, *Geology*, 25, 49–52, 1997.
- [57] Knies, J., C. Vogt, and R. Stein, *Late Quaternary growth and decay of the Svalbard/Barents Sea ice sheet and paleoceanographic evolution in the adjacent Arctic Ocean*, *Geo Mar. Lett.*, 18(3), 195–202, 1999.
- [58] Darby, D. A., J. F. Bischof, and G. A. Jones, *Radiocarbon chronology of depositional regimes in the western Arctic Ocean*, *Deep Sea Res., Part II*, 44(8), 1745–1757, 1997.
- [59] Poore, R. Z., L. Osterman, W. B. Curry, and R. L. Phillips, *Late Pleistocene and Holocene meltwater events in the western Arctic Ocean*, *Geology*, 27(8), 759–762, 1999.
- [60] Hughes, T. J., G. H. Denton, and M. G. Grosswald, *Was there a late Wisconsin Arctic ice sheet?*, *Nature*, 266, 596–602, 1977.
- [61] Nørgaard-Pedersen, N., R. F. Spielhagen, et al. *Central Arctic surface ocean environment during the past 80,000 years*, *Paleoceanography*, 13(2), 193–204, 1998.
- [62] Spielhagen, R. F., and H. Erlenkeuser, *Stable oxygen and carbon isotopes in planktic foraminifers from Arctic Ocean surface sediments: Reflection of the low salinity surface water layer*, *Mar. Geol.*, 119, 227–250, 1994.
- [63] Tarasov, P. E., O. Peyron, J. Guiot, S. Brewer, V. S. Volkova, L. G. Bezusko, N. I. Dorfeyuk, E. V. Kvavadze, I. M. Osipova, and N. K. Panova, *Last Glacial Maximum climate of the former Soviet Union and Mongolia reconstructed from pollen and plant microfossil data*, *Clim. Dyn.*, 15, 227–240, 1999.
- [64] Alley, R. B., et al., *Abrupt increase in Greenland snow accumulation at the end of the Younger Dryas event*, *Nature*, 362, 527–529, 1993.
- [65] Seidov, D., and B. J. Haupt, *Simulated ocean circulation and sediment transport in the North Atlantic during the Last Glacial Maximum and today*, *Paleoceanography*, 12, 281–306, 1997.
- [66] Kuijpers, A. H., S. R. Troelstra, M. Wisse, S. H. Nielsen, and T. C. E. van-Weering, *Norwegian Sea overflow variability and NE Atlantic surface*

- hydrography during the past 150,000 years, Mar. Geol., 152, 101– 127, 1998.*
- [67] Lassen, S., E. Jansen, K. L. Knudsen, A. Kuijpers, M. Kristensen, and K. Christensen, *Northeast Atlantic sea surface circulation during the past 30– 10 14C kyr B.P., Paleoceanography, 14(5), 616– 625, 1999.*
- [68] Denton, G. H., and T. J. Hughes, *The Arctic Ice sheet: An outrageous hypothesis, in The Last Great Ice Sheets, edited by G. H. Denton and T. J. Hughes, pp. 437– 467, John Wiley, New York, 1981.*
- [69] Hebbeln, D., and G. Wefer, *Effect of ice coverage and ice-rafted material on sedimentation in the Fram Strait, Nature, 350, 409–411, 1991.*
- [70] Dokken, T. M., and M. Hald, *Rapid climatic shifts during isotope stages 2 – 4 in the polar North Atlantic, Geology, 27, 599– 602, 1996.*
- [71] N. Nørgaard-Pedersen, R. F. Spielhagen, H. Erlenkeuser, P. M. Grootes, J. Heinemeyer, and J. Knies *Arctic Ocean during the last glacial maximum: Atlantic and polar domains of surface water mass distribution and ice cover, Paleoceanography, 18, 2003.*
- [72] Neil Dsouza, *2007 Zonally Averaged Models with Different Parameterizations and Applications (MSc. Thesis)*